Characterization of Conventional Dendritic Cells and Macrophages in the Spleen Using the *CSF1R*-Reporter Transgenic Chickens

Kate M. Sutton[1]*, Katrina M. Morris[1], Dominika Borowska[1], Helen Sang[2], Pete Kaiser[1], Adam Balic[2] and Lonneke Vervelde[1]

[1] *Division of Infection and Immunity, The Roslin Institute, University of Edinburgh, Edinburgh, United Kingdom,* [2] *Division of Functional Genetics and Development, The Roslin Institute, University of Edinburgh, Edinburgh, United Kingdom*

The spleen is a major site for the immunological responses to blood-borne antigens that is coordinated by cells of the mononuclear phagocyte system (MPS). The chicken spleen is populated with a number of different macrophages while the presence of conventional dendritic cells (cDC) has been described. However, a detailed characterization of the phenotype and function of different macrophage subsets and cDC in the chicken spleen is limited. Using the *CSF1R*-reporter transgenic chickens (*CSF1R*-tg), in which cells of the MPS express a transgene under the control elements of the chicken *CSF1R*, we carried out an in-depth characterization of these cells in the spleen. Immunohistological analysis demonstrated differential expression of MRC1L-B by periarteriolar lymphoid sheaths (PALS)-associated *CSF1R*-tg$^+$ cells. In the chicken's equivalent of the mammalian marginal zone, the peri-ellipsoid white-pulp (PWP), we identified high expression of putative CD11c by ellipsoid-associated cells compared to ellipsoid-associated macrophages. In addition, we identified a novel ellipsoid macrophage subset that expressed MHCII, CD11c, MRC1L-B, and CSF1R but not the *CSF1R*-tg. In flow cytometric analysis, diverse expression of the *CSF1R*-tg and MHCII was observed leading to the categorization of *CSF1R*-tg cells into *CSF1R*-tg^{dim} MHCII$^{inter-hi}$, *CSF1R*-tg^{hi} MHCII^{hi}, and *CSF1R*-tg^{hi} MHCII^{inter} subpopulations. Low levels of CD80, CD40, MHCI, CD44, and Ch74.2 were expressed by the *CSF1R*-tg^{hi} MHCII^{inter} cells. Functionally, *in vivo* fluorescent bead uptake was significantly higher in the *CSF1R*-tg^{hi} MHCII^{hi} MRC1L-B$^+$ cells compared to the *CSF1R*-tg^{dim} and *CSF1R*-tg^{hi} MHCII^{inter} MRC1L-B$^+$ subpopulations while LPS enhanced phagocytosis by the *CSF1R*-tg^{hi} MHCII^{inter} subpopulation. The analysis of bead localization in the spleen suggests the presence of ellipsoid-associated macrophage subsets. In addition, we demonstrated the functionality of *ex vivo* derived *CSF1R*-tg$^+$ MRC1L-B^{neg} cDC. Finally, RNA-seq analysis of the *CSF1R*-tg subpopulations demonstrated that separating the *CSF1R*-tg^{hi} subpopulation into CD11c^{hi} and CD11c^{dim} cells enriched for cDC and macrophage lineages, respectively, while the *CSF1R*-tg^{hi} MHCII^{inter} subpopulation was

enriched for red pulp macrophages. However, our analysis could not define the cell lineage of the heterogeneous $CSF1R$-tg^{dim} subpopulation. This detailed overview of the MPS in the chicken spleen will contribute to future research on their role in antigen uptake and presentation.

Keywords: chicken, *CSF1R*, dendritic cells, macrophages, mononuclear phagocyte system, RNA-seq, spleen

INTRODUCTION

The vertebrate spleen is a secondary lymphoid organ and despite differences in the immune system among vertebrates, the spleens basic histological architecture and its role in filtering the blood for antigens and damaged, aged cells has been conserved during evolution from fish, amphibians, birds, and mammals. In the mammalian spleen, the afferent splenic artery branches into the central artery which is sheathed by the white pulp areas that include the T cell zones known as the periarteriolar lymphoid sheath (PALS), arterioles, and B cell follicles. The white pulp and red pulp are extensively populated with macrophages and dendritic cells (DC) with distinct origins and functions that contribute to the control of blood-borne pathogens and homeostatic processes (1). The venous system of the red pulp gives it the capacity to filter the blood and remove old erythrocytes by red pulp macrophages. Red pulp macrophages are defined by ADGRE1^{hi} (ERM1, F4/80) CD11b^{lo}/CD18 or ADGRE1^{+} CD11b/CD18^{hi} expression (2, 3). The murine splenic red pulp also contains reservoirs of monocytes that are transcriptionally similar to their blood counterparts, Ly-6C^{+} and Ly-6C^{++} cells (ADGRE1$^{-/lo}$ CD11b^{+} CD11c^{-}) that egress to sites of tissue damage (4, 5).

The main difference between rodents and primates spleen is the structure of the marginal zone (MZ) that surrounds the white pulp. In contrast to mice, the human MZ has an inner and outer region that is surrounded by a large perifollicular zone [reviewed by (6, 7)]. The MZ consists of two resident macrophages subsets, metallophilic macrophages (MMM) located at the outer margins of the MZ and MZ macrophages (MZM) located in the inner regions of the MZ. Both MZ-resident macrophages express the scavenger receptor, MARCO while MZM also express SIGN-R1 (CD209b) (8). The MMM can uptake particular blood-borne antigens and present them to DC for cross-presentation to CD8^{+} cytotoxic T cells but they are not necessary for direct T cell activation (9).

Mammalian DC are composed of two major populations: conventional DC and plasmacytoid DC (pDC). Mammalian conventional DC are further subdivided into two major populations, cDC1 and cDC2. cDC1 develop in a BATF3 and IRF8 dependent manner and are identified by their surface expression of XCR1 and CD103, respectively (10–12). In the mammalian spleen, cDC1 are located within the T cell zones of the PALS and the outer regions of the MZ (13). The IRF4-dependent cDC2 population express CD11b, SIRPα, and DEC-205 (CD205). cDC2 are a heterogeneous cell population, the definition of these is yet to be fully resolved but they have been implicated in driving Th1, Th2, and Th17 polarization (14). The third group of DC are the IRF8-, E2-2-, and SpiB-dependent CD123^{+} pDC which are the primary source of type I IFN production following viral infection (15, 16). In humans, CD141^{+} (BDCA3) and CD1c^{+} (BDCA1), and the CD303^{+} (BDCA2) cells are the equivalent of murine cDC1, cDC2, and pDC subsets, respectively (17). In veterinary species where reagents are limited for the study of cDC and macrophage subsets, the identification of MPS cell ontogeny and cell type identity has been determined by specific gene expression patterns. For example, comparative genome analysis has identify homologous of cDC1 and cDC2 in sheep and pigs (18, 19), and cattle (20, 21). In the chicken, gene expression patterns have identified subsets of monocytes in the blood, resident tissue macrophages and cDC in the liver and spleen (22, 23).

The basic structure of the chicken spleen resembles it mammalian counterpart, with morphologically defined white pulp and red pulp regions. The white pulp contains the PALS and peri-ellipsoid white-pulp (PWP) which surround the penicillar capillaries. The PWP is analogous to the mammalian marginal zone. The ellipsoid, more commonly known as the capsule of Schweigger-Seidel (CSS) in mammals, is embedded within the PWP. The PWP contains three distinct cell populations, the ellipsoid-associated cells (EAC) and B cells intermingled with ellipsoid-associated macrophages (EAM). Studies have demonstrated the ability of EAC to retain antigen at their cell surface to either provide the antigen to the EAM or for transport to the PALS where they develop into FDC (24–28). Mannose receptor C1-like B (MRC1L-B, recognized by KUL01) is one of five orthologs of mammalian MRC1 (206) and a key mononuclear phagocytic cell marker in lymphoid and non-lymphoid tissues in chickens (29, 30). A previous comparative genomic analysis showed that splenic cDC lack MRC1L-B expression (23). However, there is limited research on the function and location of cDC, and the phenotype, function, and transcriptome of PALS-, PWP-, and red pulp-associated cells of the MPS in the chicken spleen.

The development, maintenance, and proliferation of cells of the MPS are dependent upon signals from CSF1 through its receptor, CSF1R (31) while DC require signals from FLT3L and its receptor, FLT3 (32). The tools to study the chicken MPS have been improved by the generation of the $CSF1R$-reporter transgenic chickens, in which a transgene is expressed under the control of the $CSF1R$-promoter and Fms-intronic regulatory element (FIRE) (33). These reporter chickens have contributed to the characterization of yolk-sac-derived macrophages, monocytes, and resident tissue mononuclear phagocytic cells (33–36). In this study, we utilize the $CSF1R$-reporter transgenic chickens to demonstrate the heterogeneity of the MPS in the

spleen. We show that the spleen contains at least three *CSF1R*-tg[+] subpopulations that diversely express *CSF1R*-tg, MHCII, MRC1L-B, and CD11c along with other macrophage markers. We also identified a *CSF1R*-tg[neg] macrophage population that express CSF1R protein in the PWP and demonstrate their ability to uptake beads *in vivo*. Furthermore, *in vivo* antigen uptake lead to the discovery of the diverse expression of the *CSF1R*-tg in EAM in the PWP. In addition, we demonstrate the phagocytic ability of cDC *ex vivo*. Finally, using RNA-seq we demonstrate that separation of the *CSF1R*-tg^{hi} MHCII^{hi} subpopulation into CD11c^{hi} and CD11c^{dim} subsets, enriches for genes associated with cDC and macrophage lineages while the gene signatures characteristic of red pulp macrophages are enriched in *CSF1R*-tg[hi] MHCII[inter] subpopulation. Future experiments will address the cDC-T cell interactions and the role of various cells of the splenic MPS in antigen-uptake and presentation.

MATERIALS AND METHODS

Chickens

CSF1R-reporter transgenic (33) and non-transgenic Hy-Line birds (Hy-Line Brown) between the ages of 4–8 weeks of age were provided by the National Avian Research Facility (NARF), Edinburgh, U.K. Unvaccinated chickens were reared in floor pens with access to water and food *ad-libitum*.

Isolation of Splenocytes

Spleens were aseptically removed and stored in PBS on ice. Spleens were homogenized using PYREX® Potter-Elvehjem glass tissue grinder and passed through 70 μm cell strainer (Corning®). Cells were overlaid on Histopaque (1.077 g, Sigma-Aldrich) and the interface and cell layer above were retrieved and washed twice with calcium and magnesium free PBS (pH 7.4). Cells were counted and stained at 1×10^6 cells for flow cytometric analysis.

In vitro Cell Cultures

Splenocytes were cultured at 20×10^6 cells/mL in complete media [RPMI supplemented with 10% heat-inactivated fetal bovine serum (FBS), 100 IU of penicillin, 100 μg of streptomycin (Gibco), 2 mM/mL L-glutamine (Life Technologies), and 200 ng/mL of recombinant chicken CSF1-Fc (35)]. After 24 h, non-adherent cells were removed and adherent cells were treated with TrypLE express (ThermoFisher) and reseeded at 5×10^5 cells in 24-well plates (Corning) in complete media. Cells were incubated at 41°C, 5% CO_2. Twenty-four hours later, cells were stimulated with pHrodo[TM] Red labeled Zymosan or *E. coli* bioparticles[TM], unlabeled or LPS labeled 1 μm FluoSpheres® beads (ThermoFisher) (10:1 ratio of particles/beads to cells) at 41 or 4°C. To inhibit actin polymerization, cells were treated with Cytochalasin D (Cayman Chemical) for 10 min prior to addition of the model antigens. Three hours post-treatment, ice-cold PBS was added to each well and cells were collected using TrypLE express (Gibco) for flow cytometric analysis. For immunostaining of *in vitro* cultured cells, 13 mm circular cover slips (ThermoFisher) were placed in 24-well plates and cultured as described above.

Immunostaining of Tissue Sections

For histological analysis, spleens were immediately flash frozen over liquid nitrogen or fixed in 4% paraformaldehyde (PFA/PBS) for 3 h and infused overnight with 30% sucrose (Sigma-Aldrich) at 4°C. All samples were stored at −80°C until use. Tissue sections were cut at 7 μm (Leica CM1900) and mounted on SuperFrost Plus[TM] slides (ThermoFisher) and air-dried overnight at RT after which samples were stained immediately or stored at 4°C until use. Sections were blocked with goat serum (Chrondex) or heat inactivated horse serum (Sigma-Aldrich) for 30 min diluted in PBS supplemented with 0.01% Triton-X and 0.5% BSA (Sigma-Aldrich). Tissue samples were stained with antibodies outlined in **Table 1** for 2 h at RT followed by secondary antibodies, rabbit poly anti-GFP-Alexa Fluor 488®, goat anti-mouse Alexa Fluor 568® IgG1, goat anti-mouse Alexa Fluor 647®IgG1/IgG2a, goat anti-mouse Alexa Fluor 568® IgG1 (ThermoFisher) and counterstained with 4′,6-diamidino-2-phenylindole (DAPI) or Hoechst 33258 (Sigma-Aldrich) for 1 h at RT. Slides were mounted using ProLong[TM] Diamond Antifade mountant (ThermoFisher) and analyzed using an inverted LSM710 or 880 Zeiss confocal microscope using 405, 488, 594, and 614 nm lasers, 40X or 63X Nikon oil lenses and captured using ZEN 2012 (Black Edition) software and analyzed using ZEN 2012 (Blue Edition).

Flow Cytometry and Flow Activated Cell Sorting

Splenocytes were stained using antibodies described in **Table 1**. Briefly, cells were incubated for 20 min on ice with primary antibodies diluted in Flow Buffer (PBS supplemented with 0.5% BSA and 0.01% sodium azide Sigma-Aldrich). Cells were then incubated with secondary antibodies for 20 min on ice. For multi-color flow cytometry, antibodies were conjugated using Lightning-Link[TM] (Novus Biologicals) with Alexa Fluor®647, APC-Cy[TM]7, PerCp-Cy[TM]5.5, and PE-Cy[TM]7 according to the manufacturer's instructions. All conjugated antibodies were titrated and tested for similar staining patterns observed using the unconjugated antibodies. For each experiment, live/dead cells were discriminated by the addition of SYTOX® Blue Dead Cell Stain (ThermoFisher) before cell analysis. Immuno-phenotyping of cells was carried out using BD LSRFortessa[TM] (BD Biosciences, UK) configured with 405, 488, 561, and 640 nm laser with 16 filters. Cells were sorted using BD FACS ARIA IIIu (BD Biosciences). All data was captured via BD FACSDiva[TM] Software v8.0.1 (BD Biosciences) and analyzed post-flow using FlowJo (Tree Star v10.0.2). Compensation was achieved using BD anti-mouse IgGκ compensation beads (BD Biosciences) for each flurochrome. Cell gating was carried out using cells from non-transgenic Hy-Line chickens and fluorescence minus one (FMO) controls. At least 50.000–100.000 live, single cell events were captured for analysis.

Intravenous Bead and Liposome Administration

One μm FluoSpheres® beads (ThermoFisher) were labeled with *E. coli* LPS 055:B5 (Sigma-Aldrich) as previously described (48).

TABLE 1 | Antibodies used for confocal microscopy and flow cytometry analysis.

Antibody (clone)	Antigen	Product info.	References	Cellular distribution
Mouse anti-chicken MHCII (2G11) IgG1	MHCII	Southern Biotech	(37)	B cells, macrophages, DC, low levels in T cells
Mouse anti-chicken MHCII (TAP1) IgG2a	MHCII	DSHB[a]	(38)	B cells, Macrophages, DC, low levels in T cells
Mouse anti-chicken MHCI (F21-21) IgG1	MHCI	Southern Biotech	(39)	Nucleated cells
Mouse anti-chicken CD1.1 (CB3) IgG1	CD1.1	Southern Biotech	(40, 41)	B cells, cDC
Mouse anti-chicken CD40 (IG8) IgG2a	CD40	In house	(42)	B cells, monocytes, macrophages, DC
Mouse anti-chicken CD80 (DC7) IgG2a	CD80	In house	(42)	B cells, monocytes, macrophages, DC
Mouse anti-chicken KUL01 IgG1	MRC1L-B	Southern Biotech	(29)	Monocytes and macrophages
Mouse anti-chicken K1 IgG2a	Unknown	Kind gift from Härtle, S. LMU. Germany	(43)	Monocytes, thrombocytes
Mouse anti-chicken CD11c (8F2) IgG1	Putative CD11c	Kind gift from Härtle, S. LMU. Germany	(42)	Mononuclear phagocytic cells
Mouse anti-chicken CVI-ChNL-68.2 IgG1	unknown	Prionics	(25)	Ellipsoid-associated cells
Mouse anti-chicken CVI-ChNL-74.2 IgG1	unknown	Prionics	(24)	Subpopulation splenic macrophages
Mouse anti-chicken chB6 (AV20) IgG1	Bu1	Southern Biotech	(44)	B cells, subpopulation splenic macrophages
Mouse anti-chicken CD44 (AV6) IgG1	CD44	BioRad	(45)	Macrophages, B cells
Mouse anti-chicken CD8α (3–298) IgG2b	CD8α	Southern Biotech	(46)	T cells, NK cells
Mouse anti-chicken LEP100 (IgG1)	LAMP1	DSHB[a]	(47)	Lysosomal membrane

[a] DSHB, Developmental Studies Hybridoma Bank.

Chickens between the ages of 5–8 weeks were intravenously administered with 100 μl of beads in PBS containing 3.6 × 10^9 0.5 μm or unlabeled or LPS labeled 1 μm carboxylate FluoSpheres® beads (ThermoFisher) or 100 μl of PBS- or clondronate-encapsulated liposomes (5 mg Liposoma, Europe) via the wing vein. Chickens were culled 3 h (beads) or 3 days (liposome) post-administration by cervical dislocation. Half of the spleen was prepared for immunohistology and the other half prepared for flow cytometric analysis. Ten thousand live, single cell events in the bead$^+$ gate were captured for analysis.

RNA-Seq Sample Preparation

Splenocytes were prepared as described above and sorted from five *CSF1R*-eGFP chickens at 7 weeks of age. Cells were sorted under low speed using an 80 μm diameter nozzle into 1.5 mL Eppendorf tubes at 4°C. Following cell sort, samples were pelleted at 400 *g* for 3 min and lysed using RLT buffer (Qiagen) supplemented with β-mercaptoethanol and stored at −20°C until use. RNA was purified using RNA Micro extraction kit according to the manufacturer's instructions (Qiagen). RNA concentration and quality was measured using High Sensitivity RNA Screen Tape System (Agilent). All samples were used with a RIN ≥7. cDNA was transcribed using Ovation® RNA-Seq System V2 (NuGen) according to the manufacturer's instructions. cDNA quality and quantity was analyzed using D1000 Screen Tape System (Agilent). RNA-seq was carried using TruSeq DNA Nano (350 bp insert) library preparation, sequencing using Illumina HiSeq4000 and data generation and preliminary analysis was carried out by Edinburgh Genomics, The University of Edinburgh, U.K.

RNA-Seq Analysis

Reads were trimmed using Cutadapt (version 1.9.dev2) (49) for quality at the 3' end using a quality threshold of 30 and for adapter sequences of the TruSeq DNA Nano kit. Reads after trimming were required to have a minimum length of 50 bp. Reads were aligned against the *Gallus gallus* 5.0 genome from Ensembl using STAR (50). Raw counts for each annotated gene were obtained using the feature counts software [version 1.5.2; (51)]. Reads were normalized using the weighted trimmed mean of M-values method (52). Differential gene expression analysis was performed within the Bioconductor edgeR package [version 3.16.5; (52)]. For differential analysis the raw counts table was filtered to remove genes consisting predominantly of near-zero counts, filtering on counts per million (CPM) to avoid artifacts due to library depth. Statistical assessment of differential expression was carried out with the likelihood-ratio test. Contrasts specified were each pair of sorted cell populations. Differentially expressed genes were defined as those with a false-discovery rate (FDR) <0.05 and log2 fold-change (FC) >2. Heatmaps were constructed using normalized gene counts in R using the pheatmap package (v. 1.0.10; https://CRAN.R-project.org/package=pheatmap). To statistically test whether mammalian immune cell transcriptional signatures were enriched in each chicken cell population we used a pairwise gene set enrichment analysis (GSEA) approach using the BubbleGum software for statistical calculations and graphical output (53). The chicken data was compared to mouse data as more spleen specific gene sets were available than for other species. We used mouse immune cell-specific gene sets developed previously (23, 54), which are comprised of genes that show at least 1.5-fold higher expression in the cell population of interest compared to other immune cells. The gene sets used were for splenic T cells, B

cells, cDC1, pDC, cDC vs. monocytes/macrophages (Mo/Mp), Mo/Mp vs. cDC. In addition, we used blood derived mouse cMo, ncMo, and MoDC data sets. Sequences have been submitted to European Nucleotide Archive (ENA) under the accession number PRJEB40127.

Statistical Analysis

All data was analyzed for normality using Shapiro-Wilk test and non-parametric analysis was performed using GraphPad Prism 8 (GraphPad, USA). Differences between the groups were statistically evaluated by the non-parametric Mann-Whitney or Kruskal-Wallis test adjusted for *post-hoc* analysis. For all statistical analysis, $P < 0.05$ were considered significant.

RESULTS

Splenic PALS-Associated *CSF1R*-tg$^+$ Cells Do Not Uniformly Express MRC1L-B

Whole mount microscopic analysis of the *CSF1R*-tg chicken spleen demonstrates the high density of *CSF1R*-tg$^+$ cell sheaths within the splenic PALS and the PWP (**Figure 1A**). A microscopic overview of *CSF1R*-tg and CD11c expression, using the putative anti-chicken CD11c monoclonal, 8F2, demonstrates low expression levels of CD11c in the PALS and PWP regions and high levels of expression in cells of the red pulp (**Figure 1B** and **Supplementary Figure 1**). At the origin of the PALS, *CSF1R*-tg$^+$ cells that surround the central artery express the chicken monocyte/macrophage markers, Ch74.2, which binds to an unknown epitope, MHCII and mannose receptor C1-like B [MRC1L-B formally known as KUL01, **Figures 1C,D**; (30)]. *CSF1R*-tg$^+$ interdigitating cells are scattered throughout the PALS and express Ch74.2 and MHCII, while they differentially express MRC1L-B (**Figures 1C,D**). A lack of MRC1L-B expression is a hallmark for cDC in the chicken spleen (21). At the bifurcation of the central artery resides the GCs that contain *CSF1R*-tg$^+$ follicular dendritic cells (FDC) that lack Ch74.2, MHCII, and MRC1L-B expression (**Figures 1C,D**) and bind IgY (**Figure 1E**). ChB6$^+$ B cells are located within the GC and in the PWP where they form a ring around the ellipsoid (**Figure 1F**). PWP-associated chB6$^+$ B cells are intermingled with ellipsoid-associated macrophages (EAM) that express the *CSF1R*-tg, Ch74.2, MHCII, and MRC1L-B (**Figures 1G,H**). Closer analysis of the red pulp demonstrated that not all red pulp-associated *CSF1R*-tg$^+$ cells express Ch74.2 (**Figure 1G** image insert) but they strongly express MRC1L-B (**Figure 1H**). Within the inner regions of the PWP are EAC that express the *CSF1R*-tg (33) and can also be identified using the monoclonal Ch68.2 which binds to an unknown epitope [**Figure 1I**; (25)]. The *CSF1R*-tg$^+$ expression demonstrates that cells of the splenic MPS differentially express MRC1L-B and help to distinguish cDC in the chicken spleen.

A *CSF1R*-tg^{neg} Subpopulation Is Located in the Ellipsoid and Express CSF1R Protein

The PWP is structurally defined as the region from the discontinuous basement membrane of the penicilliform capillary that harbors supportive cells surrounded by the capsule of the Schweigger-Seidel sheath [**Figure 2A**; (28)]. The ellipsoid, embedded within the PWP, is the filtering apparatus of the spleen and represents a key component of chicken splenic lymphoid system. Using high-resolution confocal analysis, the *CSF1R*-tg$^+$ EAC were observed anchored to the ellipsoid, positioned to be the primary cells to encounter blood-borne antigens (**Figure 2B**). Double staining of spleen sections with Ch68.2 and MHCII, lead to the identification of a ring of Ch68.2^{neg} MHCII$^+$ cells within the ellipsoid that were found to be *CSF1R*-tg^{neg} (**Figure 2C**). Although these cells lack transgene expression, they were found to express the CSF1R protein (**Figure 2D**) and also expressed MRC1L-B and CD11c (**Figures 2E,F**). To distinguish these cells from EAM we denominate them as ellipsoid macrophages (EM). The expression of MHCII by the EAC was not easily identifiable. In some instances, intracellular MHCII staining was observed in the EAC whereas surface expression was difficult to demonstrate which may suggest a lack of MHCII surface expression or expression levels being undetectable via confocal microscopy (**Figures 2C–E** and **Supplementary Figure 2**). We also observed lower levels of CD11c expression by the EAM compared to the EAC (**Figure 2D**). LAMP1 expression was observed throughout the PWP and its expression was found within the EAM, EAC, and the EM cell populations (**Figure 2G**). Overall, our analysis show that a network of EM reside within the inner margins of the ellipsoid that express a number of chicken macrophage markers and the CSF1R protein but not the *CSF1R*-tg.

The Chicken Spleen Contains Cells of the MPS That Diversely Express the *CSF1R*-tg, MHCII MRC1L-B, and CD11c

We next analyzed the phenotype of splenic cells of MPS from the *CSF1R*-tg chickens using flow cytometry. After gating the cells based on size/granularity and the removal of cell debris, doublets, and dead cells (**Supplementary Figure 3**), typically five subpopulations were observed based on their *CSF1R*-tg and MHCII expression patterns (**Figure 3A**). Firstly, the *CSF1R*-tg^{neg} population was gated into MHCII^{dim} (Gate 1) and MHCII^{hi} subpopulations (Gate 2). The *CSF1R*-tg$^+$ subpopulation made up ~5% of the total live cell population in which three distinct subpopulations were observed based on their *CSF1R*-tg$^+$ and MHCII expression levels (Gates 4-6). Histogram overlays of the *CSF1R*-tg$^+$ subpopulations demonstrated diversity of *CSF1R*-tg and MHCII expression (**Figure 3B**). The median fluorescent intensity (MFI) of *CSF1R*-tg and MHCII expression levels indicated that cells within Gate 4 had significantly lower levels of *CSF1R*-tg expression compared to cells in Gates 5 and 6. This subpopulation expressed intermediate to high levels of MHCII (**Figure 3C**) and were named *CSF1R*-tg^{dim} MHCII$^{inter−hi}$ subpopulation. Cells within Gates 5–6 expressed high levels of the *CSF1R*-tg and differ in their MHCII expression levels. Cells in Gate 5 expressed significantly higher levels of MHCII compared to cells in Gate 6 and hence named the *CSF1R*-tg^{hi} MHCII^{hi} (Gate 5) and *CSF1R*-tg^{hi} MHCII^{inter} (Gate 6) subpopulations, respectively. In terms of size and granularity, the
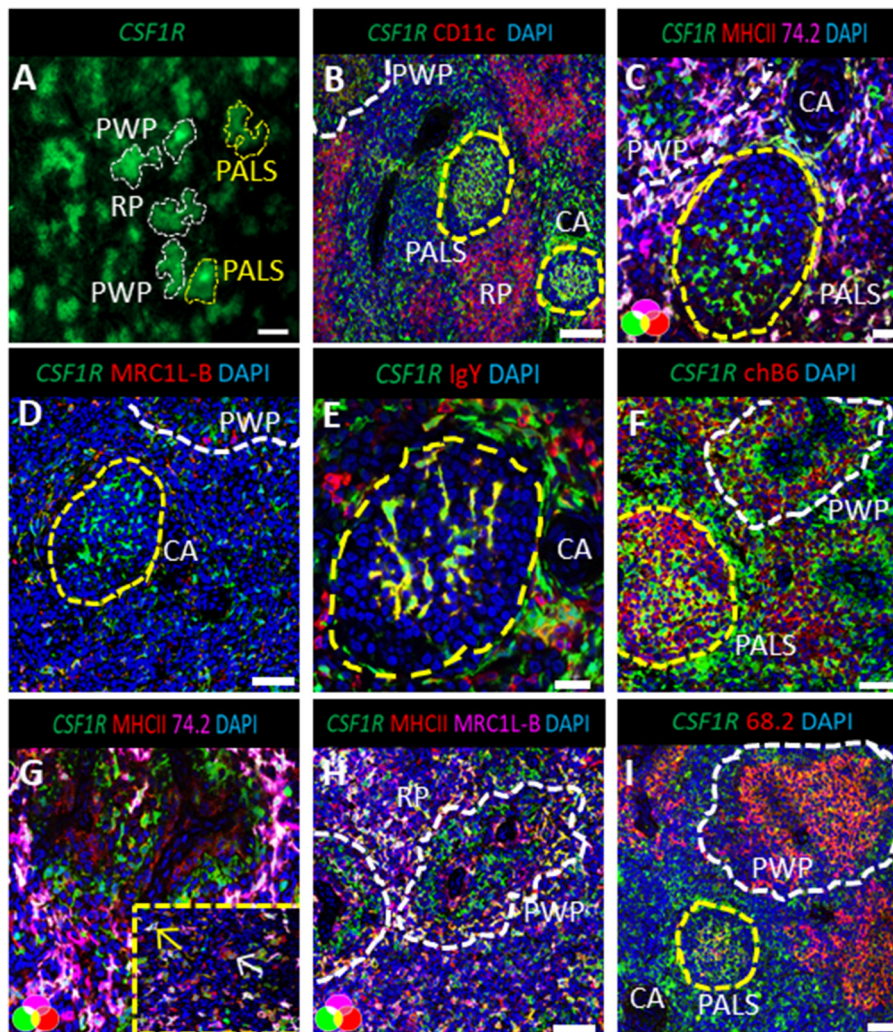
FIGURE 1 | *CSF1R*-tg$^+$ mononuclear phagocytes differentially express MRC1L-B and CD11c in the spleen. The white pulp of the chicken spleen consists of two morphologically distinct areas, the peri-arteriolar lymphoid sheaths (PALS) that surround the central artery (CA) and the peri-ellipsoid white pulp (PWP) surrounding the penicillary capillaries. **(A)** Whole mount microscopic analysis of the spleen demonstrates the abundance of *CSF1R*-tg$^+$ cells in the PALS and PWP; **(B)** CD11c is differentially expressed across the PALS and PWP and high concentrations of CD11c^{hi} cell sheaths were observed in the red pulp (RP); **(C)** the chicken macrophage marker, Ch74.2, is expressed by a majority of the *CSF1R*-tg$^+$ MHCII$^+$ PALS-associated mononuclear phagocytic cells in contrast to the FDC and the EAC in the PWP; **(D)** *CSF1R*-tg$^+$ cells surrounding the CA express MRC1L-B while some scattered *CSF1R*-tg$^+$ PALS-associated mononuclear phagocytic cells lack MRC1L-B expression which is also observed in FDC; **(E)** FDC and plasma cells express IgY; **(F)** GC are packed with chB6$^+$ B cells and chB6$^+$ B cells surround the ellipsoid in the PWP; **(G)** in the PWP, Ch74.2$^+$ EAM reside in the outer regions of the PWP and in the red pulp, not all *CSF1R*-tg$^+$ cells express this chicken macrophage marker [insert image of Ch74.2$^+$ (yellow arrow) and Ch74.2^{neg} (white arrow) staining in red pulp macrophages]; **(H)** EAM express MHCII and MRC1L-B in contrast to the EAC; **(I)** *CSF1R*-tg is expressed by the Ch68.2$^+$ EAC. Yellow dashed circles indicate GC, white dashed lines indicates the PWP. Data is representative of five *CSF1R*-eGFP transgenic chickens at 5–6 weeks of age. Images **(B-D-F-G-I)** are 2X2 tiled images with 100 µm scale bars and 50 µm scale bars for images **(C,E)**.

CSF1R-tg^{hi} MHCII^{inter} subpopulation was more homogenous than the *CSF1R*-tg^{dim} MHCII$^{inter-hi}$ and *CSF1R*-tg^{hi} MHCII^{hi} subpopulations (**Figure 3D**).

Using the gating strategy outlined in **Figure 3A**, we next analyzed the expression of MRC1L-B and CD11c across each subpopulation (Gates 1–6, **Figure 3E**). We found no MRC1L-B$^+$ cells within the *CSF1R*-tg^{neg} MHCII^{dim} subpopulation and they were largely CD11c$^+$ (**Figure 3E**). Within the *CSF1R*-tg^{neg} MHCII^{hi} subpopulation a small percentage of MRC1L-B^{hi} CD11c^{hi} cells were observed (**Figure 3E**), which may represent the *CSF1R*-tg^{neg} EM observed in the ellipsoid

via immunohistology. The *CSF1R*-tg^{dim} MHCII$^{inter-hi}$ and *CSF1R*-tg^{hi} MHCII^{hi} subpopulations were very heterogeneous, consisting of MRC1L-B^{hi} CD11c^{hi}, MRC1L-B^{inter} CD11c$^{inter-hi}$ cells while a third subset expressed low level or no MRC1L-B and high levels of CD11c, making up around 30–35% of the cell population in each of these subpopulations, respectively (**Figure 3E** and **Supplementary Figure 4**). The *CSF1R*-tg^{hi} MHCII^{inter} subpopulation were homogenous in their MRC1L-B and CD11c (88%) expression and lacked the MRC1L-B^{inter} cells observed in the *CSF1R*-tg^{dim} MHCII$^{inter-hi}$ and *CSF1R*-tg^{hi} MHCII^{hi} subpopulations (**Figure 3E**). Histogram
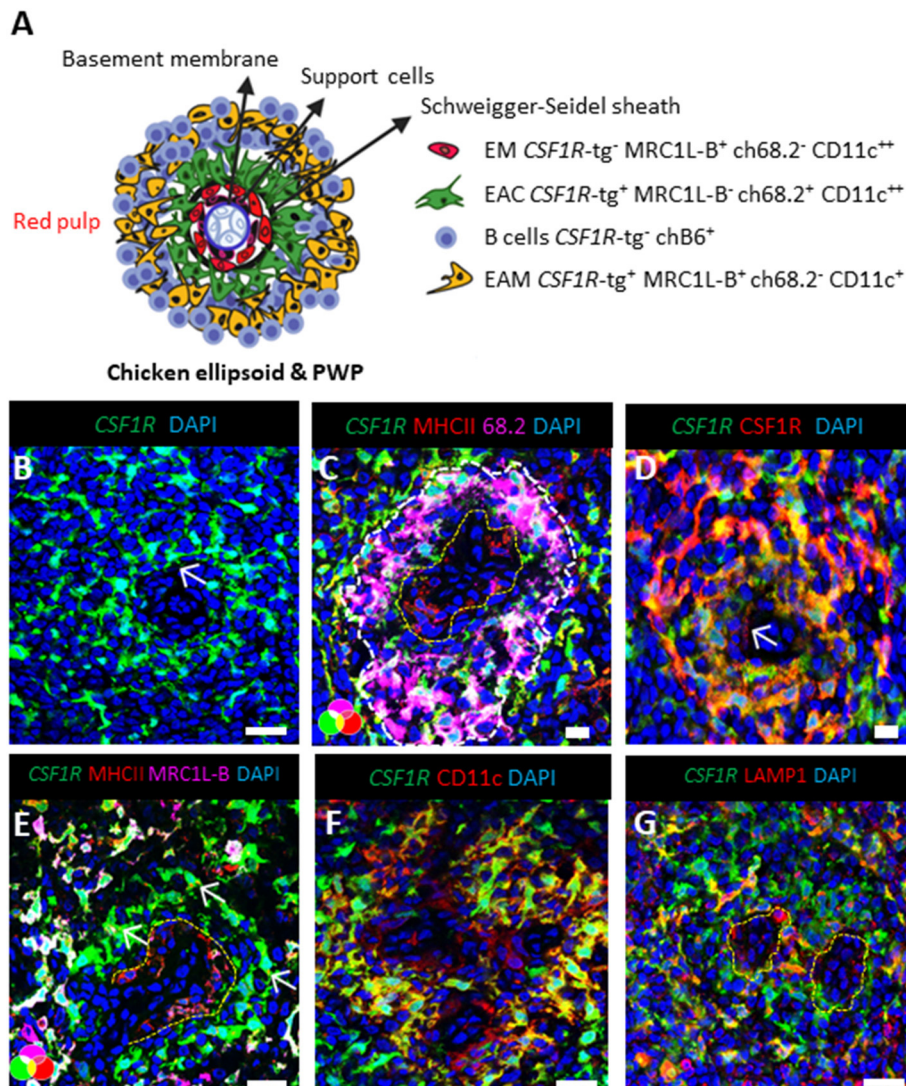
FIGURE 2 | The ellipsoid contains *CSF1R*-tg negative cells that co-express chicken macrophage related markers. **(A)** Schematic overview of the chicken PWP, ellipsoid and associated cells, EC; ellipsoid macrophages, EAC; ellipsoid-associated cells, EAM: ellipsoid-associated macrophages; **(B)** confocal analysis of the PWP demonstrates the dendrites of the *CSF1R*-tg$^+$ EAC cells protruding into the ellipsoid (white arrow); **(C)** MHCII and Ch68.2 staining demonstrates the presence of *CSF1R*-tg^{neg} MHCII$^+$ Ch68.2^{neg} cell population named ellipsoid macrophages (EM) that are located within the ellipsoid; **(D)** CSF1R is expressed by the *CSF1R*-tg^{neg} EM; **(E)** in contrast to EM and EAM, EAC lack MRC1L-B expression; **(F)** EAC and EM express high levels of CD11c in contrast to the EAM; **(G)** LAMP1 is expressed by all *CSF1R*-tg$^+$ and *CSF1R*-tg^{neg} cells in the PWP. Yellow lines outline the location of the EM. Data is representative of five *CSF1R*-eGFP transgenic chickens at 5–6 weeks of age. Scale bars for images **(B,E–G)** are 100 μm and images **(C,D)** are 50 μm.

overlays of MRC1L-B and CD11c expression in each *CSF1R*-tg subpopulations shows the uniform level of expression of these markers in the *CSF1R*-tg^{hi} MHCII^{inter} subpopulation compared to the *CSFR*-tg^{dim} MHCII$^{inter−hi}$ and *CSF1R*-tg^{hi} MHCII^{hi} subpopulations (**Supplementary Figure 4**). Although numerous extraction approaches were carried out, we did not observed a *CSF1R*-tg$^+$ MHCII$^{neg/low}$ MRC1L-B^{neg} CD11c$^+$ phenotype that would represent the EAC and FDC subpopulations in the chicken spleen. This may reflect the low survival rates of these cells post-extraction or they may express low levels of MHCII and are represented in the *CSF1R*-tg$^+$ subpopulations. Even with these limitations, our complex multicolor flow cytometric

analysis demonstrates the existence of at least three *CSF1R*-tg$^+$ subpopulations in the chicken spleen that diversely express the *CSF1R*-tg, MHCII, MRC1L-B, and CD11c.

The *CSF1R*-tg^{hi} MHCII^{inter} Subpopulation Expresses Low Levels of CD80, CD40 and MHCI, CD44, and Ch74.2

We next analyzed the expression of co-stimulatory molecules, CD80, CD40, and MHCI and CD44, across the three *CSF1R*-tg$^+$ MHCII$^+$ subpopulations by flow cytometry (**Figure 4A**). Histogram overlays indicated that the *CSF1R*-tg^{hi} MHCII^{inter}
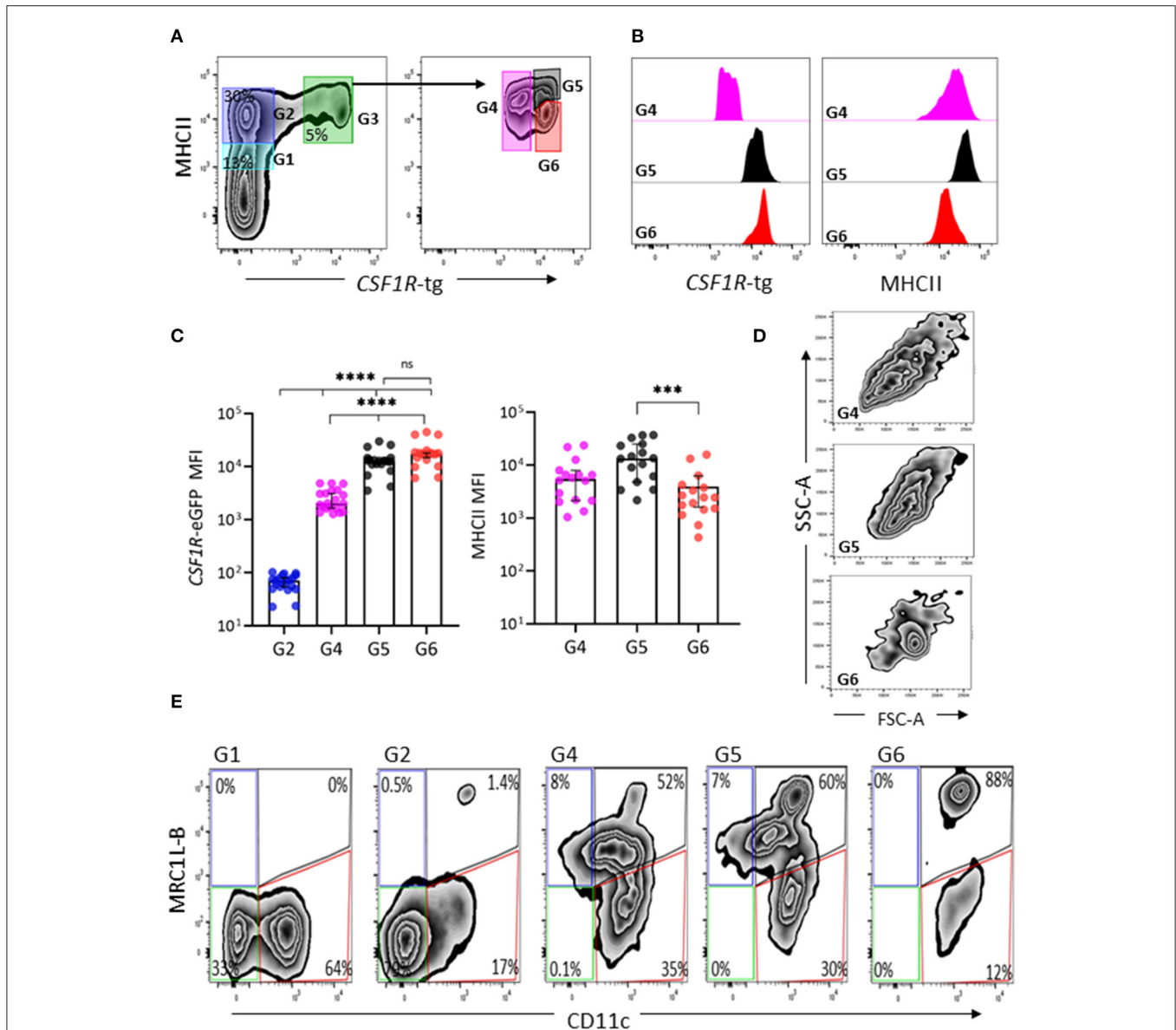
FIGURE 3 | *CSF1R*-tg and MHCII are diversely expressed by *CSF1R*-tg⁺ cells. Splenic live, single cells could be separated based on their diverse *CSF1R*-tg and MHCII expression by flow cytometry. **(A)** The *CSF1R*-tg negative populations were gated into MHCII^dim [Gate (G1)] and MHCII^hi (G2) subpopulations. By applying a gate to the *CSF1R*-tg⁺ population (G3), the differential expression of the transgene and MHCII could be observed. Three *CSF1R*-tg⁺ subpopulations were separated into *CSF1R*-tg^dim MHCII^inter−hi (G4) and two *CSF1R*-tg^hi cell subpopulations; *CSF1R*-tg^hi MHCII^hi (G5) and *CSF1R*-tg^hi MHCIIinter (G6) subpopulations; **(B)** Representative histograms of *CSF1R*-tg and MHCII expression levels in the *CSF1R*-tg⁺ subpopulations (G4-6); **(C)** The median fluorescent intensity (MFI) analysis across 20 *CSF1R*-eGFP chickens shows the consistent difference of *CSF1R*-tg and MHCII expression. Error bars indicate 95% confidence intervals, Asterisks indicate statistical significance ($P < 0.05$); **(D)** The *CSF1R*-tg^hi MHCII^inter subpopulation has more uniformed cell size and granularity pattern compared to the *CSF1R*-tg^dim MHCII^inter−hi (G4) and *CSF1R*-tg^hi MHCII^hi (G5) subpopulations; **(E)** *CSF1R*-tg^hi MHCII^inter (G6) subpopulation has more uniformed expression of MRC1L-B and CD11c compared to the *CSF1R*-tg^dim MHCII^inter−hi (G4) and *CSF1R*-tg^hi MHCII^hi (G5) subpopulations. Analysis were applied to cells gated based on size/granularity, live, single cells, *CSF1R*-tg⁺ MHCII⁺ gates using FMO-1 controls. Data is representative of 5 or more independent experiments from 4-8 week old *CSF1R*-eGFP transgenic chickens.

subpopulation has lower levels of co-stimulatory molecule, CD80 and CD40, and MHCI and CD44 expression, although these differences were only significant for CD40 (**Figure 4A**). We next analyzed the expression of non-classical MHC molecule, CD1.1, the chicken monocyte/thrombocyte marker, K1, and Ch74.2 across each *CSF1R*-tg⁺ subpopulation (**Figure 4B**). A

subpopulation of CD1.1^hi cells were present in the *CSF1R*-tg^dim and *CSF1R*-tg^hi MHCII^hi subpopulations whereas *CSF1R*-tg^hi MHCII^inter cells were negative for CD1.1 expression (**Figure 4B**). The K1 marker (43) was expressed at low levels across all *CSF1R*-tg⁺ subpopulations with a small population of K1^hi cells within *CSF1R*-tg^dim MHCII^inter−hi
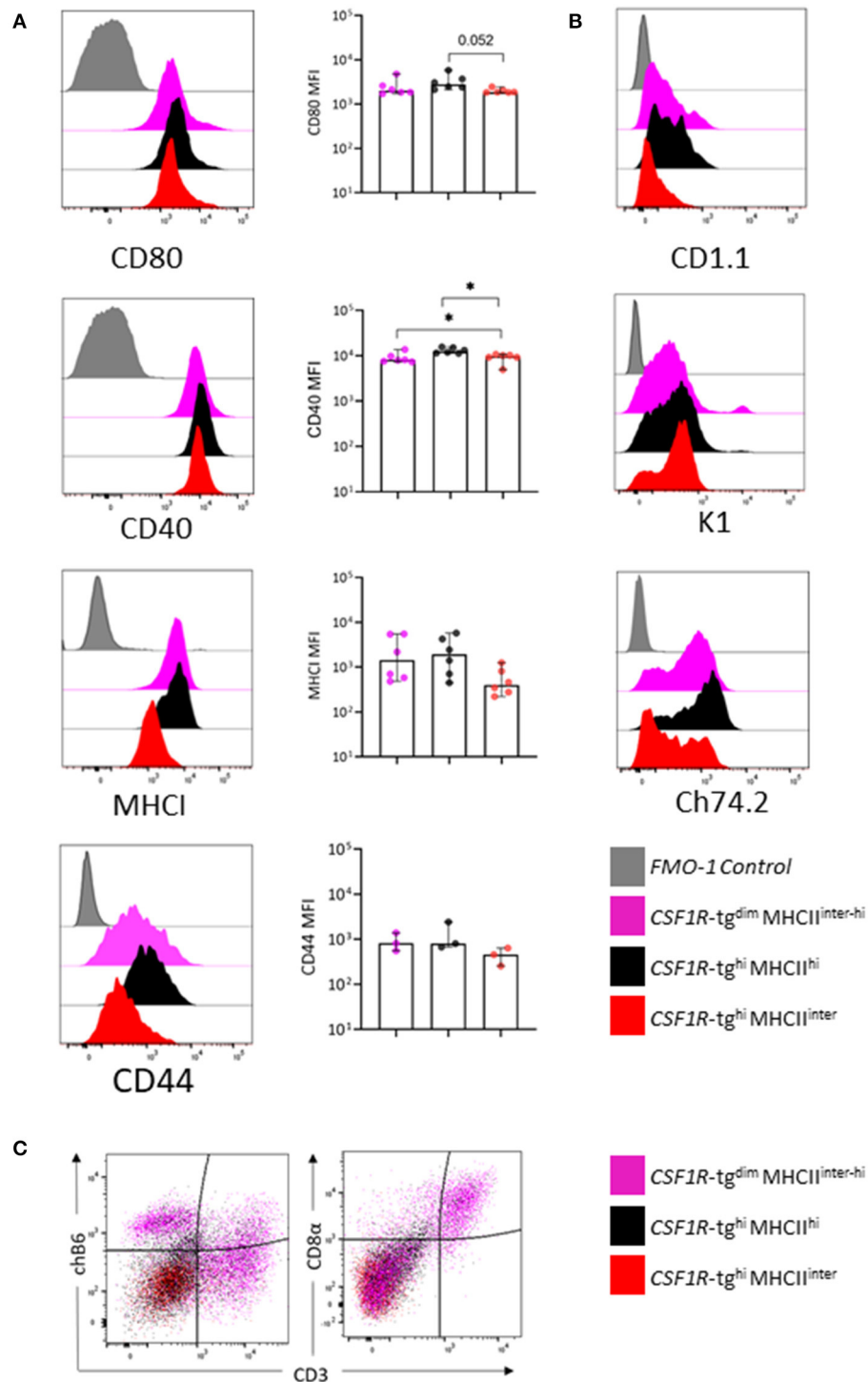
FIGURE 4 | The *CSF1R*-tg[hi] MHCII[inter] subpopulation express low levels of CD80, CD40, MHCI, CD44, and Ch74.2. The three *CSF1R*-tg[+] subpopulations were gated as outlined in **Figure 3A** and analyzed for a number of chicken mononuclear phagocytic cell markers by flow cytometry. **(A)** Representative histograms and MFI expression levels of CD80, CD40, MHCI, and CD44, across the three *CSF1R*-tg[+] subpopulations; **(B)** representative histograms of CD1.1, K1, and Ch74.2 expression across the three *CSF1R*-tg[+] subpopulations; **(C)** representative flow plots of chB6, CD3, and CD8α expression across the *CSF1R*-tg[+] subpopulations indicates that the *CSF1R*-tg[dim] MHCII[inter−hi] subpopulation express B cell and T cell markers along with macrophage markers. Gates were applied to size/granularity, live, single cells, *CSF1R*-tg[+] MHCII[+] gates using FMO controls. Data is representative of 3–6 independent experiments from 4 to 6 week old chickens. Error bars indicate 95% confidence intervals. Asterisks indicate statistical significance ($P < 0.05$).

subpopulation. The *CSF1R*-tg^{hi} MHCII^{inter} cells contained Ch74.2^{hi} and Ch74.2^{neg} cell populations whereas the *CSF1R*-tg^{dim} MHCII$^{inter-hi}$ and *CSF1R*-tg^{hi} MHCII^{inter} cells had a more uniformed expression pattern of Ch74.2 (**Figure 4B**). The chicken B cell marker, chB6, binds to a subset of splenic macrophages (55). We therefore analyzed the expression of chicken T/NK cells and B cell markers within the subpopulations and found that ChB6 label cells within the *CSF1R*-tg^{dim} subpopulation while a small population expressed CD3 and CD8α, possibly indicating the presence of T cells and NK cells along with macrophages (**Figure 4C**) The *CSF1R*-tg^{neg} MHCII^{hi} MRC1L-B$^+$ subpopulation expressed high levels of CD80, CD40, and K1 (**Supplementary Figure 5A**). We also verified the lack of CD41/61 expression in *CSF1R*-tg$^+$ cells indicating that thrombocyte contamination was not altering the expression levels of the cell markers (**Supplementary Figure 5B**). Overall, our multicolor flow cytometry analysis indicates that the *CSF1R*-tg^{hi} MHCII^{inter} subpopulation expressed lower levels of CD80, CD40, MHCI, CD44, CD1.1, and Ch74.2 compared to the *CSF1R*-tg^{dim} MHCII$^{inter-hi}$ and *CSF1R*-tg^{hi} MHCII^{hi} subpopulations.

The Phagocytosis Abilities of the *CSF1R*-tg^{hi} MHCII^{inter} Cells Are Enhanced by LPS

To determine the function of the *CSF1R*-tg$^+$ subpopulations, 5–6 week old *CSF1R*-eGFP transgenic chickens were intravenously administered 0.5 μm or unlabeled and LPS labeled 1 μm fluorescent beads. Three hours post-IV administration, the phenotype of the splenic phagocytic cells was analyzed by applying the gating strategy outlined in **Figure 3A** on the bead^{neg} cell population which was subsequently applied to the bead$^+$ cell population (**Figure 5A**). Due to low number of bead$^+$ events in the *CSF1R*-tg^{neg} MHCII^{inter} subpopulation, these cells were analyzed with the *CSF1R*-tg^{neg} MHCII^{hi} subpopulation. In the 0.5 μm bead$^+$ gate, the cell percentages of the *CSF1R*-tg^{neg}, *CSF1R*-tg^{dim} MHCII$^{inter-hi}$, and *CSF1R*-tg^{hi} MHCII^{hi} subpopulations were significantly higher compared to the *CSF1R*-tg^{hi} MHCII^{inter} subpopulation. When the MFI of the 0.5 μm beads was analyzed in each subpopulation, all *CSF1R*-tg subpopulations had statistically significant higher bead uptake compared to the *CSF1R*-tg^{neg} subpopulation (**Figure 5B**).

Next, the ability of the *CSF1R*-tg cells to phagocytose 1 μm beads was analyzed. After 3 h, the percentage of *CSF1R*-tg^{neg} cells within the 1 μm bead$^+$ gate was significantly higher compared to the *CSF1R*-tg^{dim} MHCII$^{inter-hi}$ and *CSF1R*-tg^{hi} subpopulations (**Figure 5C**). Between the *CSF1R*-tg$^+$ subpopulations, the percentage of the *CSF1R*-tg^{hi} MHCII^{hi} subpopulation was significantly higher compared to the *CSF1R*-tg^{dim} and *CSF1R*-tg^{hi} MHCII^{inter} subpopulations. The MFI analysis of the 1 μm beads show that although the *CSF1R*-tg^{dim} subpopulation was significantly underrepresented in the bead$^+$ gate, they had significantly higher bead uptake compared to the *CSF1R*-tg^{hi} MHCII^{inter} subpopulation. In addition, the *CSF1R*-tg^{neg} and *CSF1R*-tg^{hi} MHCII^{hi} subpopulations phagocytosed significantly
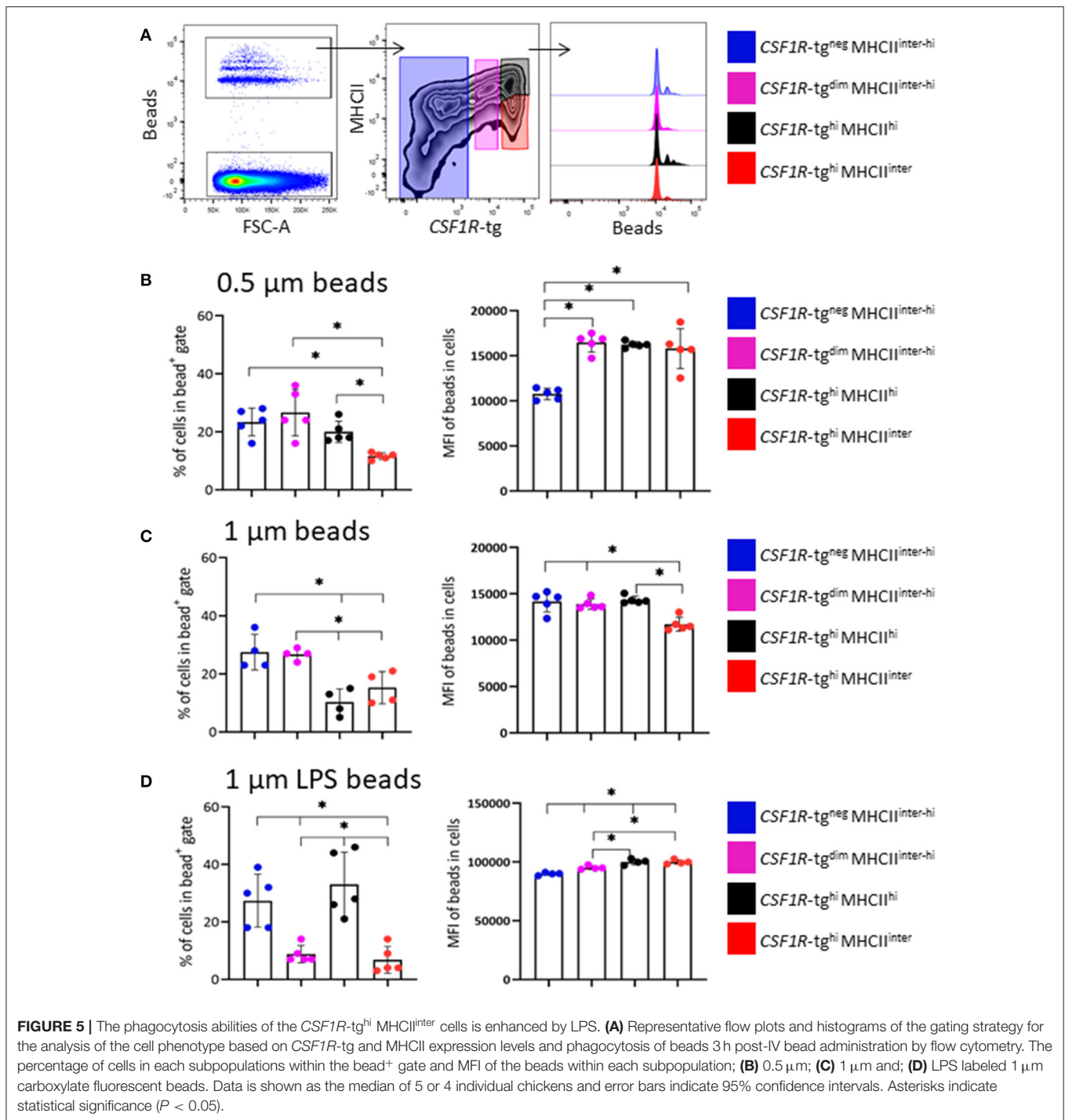
higher number of beads compared to the *CSF1R*-tg^{hi} MHCII^{inter} subpopulation (**Figure 5C**).

To determine the phagocytosis abilities of cells exposed to bacterial antigens, 1 μm beads were labeled with LPS and phagocytosis was analyzed 3 h post-IV administration. The percentages of both *CSF1R*-tg^{neg} and *CSF1R*-tg^{dim} MHCII$^{inter-hi}$ subpopulations in the bead$^+$ gate were significantly higher compared to the *CSF1R*-tg^{hi} MHCII^{hi} and *CSF1R*-tg^{hi} MHCII^{inter} subpopulations (**Figure 5D**). The MFI levels of the LPS labeled 1 μm beads were significantly higher in the *CSF1R*-tg^{hi} MHCII^{hi} and *CSF1R*-tg^{hi} MHCII^{inter} subpopulations compared to the *CSF1R*-tg^{dim} MHCII$^{inter-hi}$ subpopulation. All *CSF1R*-tg$^+$ subpopulations had significantly higher bead uptake compared to the *CSF1R*-tg^{neg} subpopulation (**Figure 5D**). *In vivo* functional analysis indicates that exposure to LPS enhances the phagocytosis of 1 μm beads by the *CSF1R*-tg^{hi} MHCII^{inter} subpopulation.

In vivo Antigen Uptake Demonstrates Diversity in the EAM in the PWP

Flow cytometric analysis demonstrated the differential expression of MRC1L-B across each of the *CSF1R*-tg$^+$ subpopulations and the existence of the *CSF1R*-tg^{neg} MRC1L-B$^+$ subpopulation (**Figure 3D**). We analyzed the percentage of MRC1L-B expressing cells in the bead$^+$ *CSF1R*-tg$^+$ and *CSF1R*-tg^{neg} subpopulations and used immunohistochemistry to analyze the location of the beads in the spleen 3 h post-administration (**Figure 6**). Firstly, we found a majority of 0.5 μm bead$^+$ *CSF1R*-tg$^+$ cells consisted of MRC1L-B expressing cells ($\sim$95%) which was significantly higher compared to the percentage of MRC1L-B$^+$ in both the 0.5 μm bead$^+$ *CSF1R*-tg^{dim} MHCII$^{inter-hi}$ and *CSF1R*-tg^{hi} MHCII^{inter} subpopulations ($\sim$75–70%). In the 0.5 μm bead$^+$ *CSF1R*-tg^{neg} subpopulation, we found that $\sim$10% of cells expressed MRC1L-B. In the unlabeled 1 μm bead$^+$ *CSF1R*-tg^{hi} MHCII^{hi} subpopulation ($\sim$98%), the percentage of MRC1L-B expressing cells was significantly higher compared to the *CSF1R*-tg^{dim} MHCII$^{inter-hi}$ and *CSF1R*-tg^{hi} MHCII^{inter} MRC1L-B subpopulations ($\sim$90–85%) while no significance difference between the *CSF1R*-tg$^+$ cells was observed after phagocytosis of LPS labeled 1 μm beads. In the *CSF1R*-tg^{neg} unlabeled and LPS labeled 1 μm bead$^+$ subpopulation, MRC1L-B expressing cells made up $\sim$50% of the cell population demonstrating the phagocytosis abilities of the EM (**Figure 6A**).

We next analyzed the location of the bead$^+$ cells in the spleen 3 h post-administration. Whole mount microscopic analysis shows that irrespective of bead size or LPS coating, beads were localized to the PWP (**Supplementary Figure 6**). Additional in depth analysis found that the 0.5 μm beads were located within the *CSF1R*-tg$^+$ Ch68.2$^+$ cells but high concentrations of beads were observed in the *CSF1R*-tg$^+$ Ch68.2^{neg} cells, which represent the EAM (**Figure 6B**i). Uptake of 1 μm beads was observed in the *CSF1R*-tg$^+$ Ch68.2$^+$ EAC but a majority of beads were associated with the *CSF1R*-tg$^+$ Ch68.2^{neg} EAM (**Figure 6B**ii). Beads were also found closely associated with chB6$^+$ cells in the ellipsoid representing the *CSF1R*-tg^{neg} MRCL1-B^{neg} bead$^+$ cell phenotype observed in flow cytometry (**Supplementary Figure 6**). Large

FIGURE 5 | The phagocytosis abilities of the *CSF1R*-tg[hi] MHCII[inter] cells is enhanced by LPS. **(A)** Representative flow plots and histograms of the gating strategy for the analysis of the cell phenotype based on *CSF1R*-tg and MHCII expression levels and phagocytosis of beads 3 h post-IV bead administration by flow cytometry. The percentage of cells in each subpopulations within the bead[+] gate and MFI of the beads within each subpopulation; **(B)** 0.5 µm; **(C)** 1 µm and; **(D)** LPS labeled 1 µm carboxylate fluorescent beads. Data is shown as the median of 5 or 4 individual chickens and error bars indicate 95% confidence intervals. Asterisks indicate statistical significance (*P* < 0.05).

deposits of LPS labeled 1 µm beads were also located in the *CSF1R*-tg[+] MRC1L-B[+] EAM compared to the *CSF1R*-tg[+] MRC1L-B[neg] EAC (**Figure 6B**iii). Due to their location in the PWP the uptake of beads by the different MRC1L-B[+] *CSF1R*-tg[+] subpopulations indicates the variable expression of the *CSF1R*-tg by EAM. Thus, *in vivo* antigen uptake demonstrates the existence of EAM subsets that differ in their *CSF1R*-tg expression and antigen uptake but not in their MRC1L-B expression.

The *CSF1R*-tg[+] MRC1L-B[neg] cDC Can Phagocytose Model Antigens

We observed a vast majority of *CSF1R*-tg[+] MRC1L-B^{neg} cells in the splenic PALS and very little in the PWP. These cells were found to be a minor population in *CSF1R*-tg[+] bead^{+} cells in the *in vivo* uptake analysis by flow cytometry while immunohistological analysis demonstrated the lack of beads in the PALS 3 h post-administration (**Supplementary Figure 6B**).

FIGURE 6 | *In vivo* functional analysis indicates diversity in the EAM. **(A)** The percentage of MRC1L-B+ cells in the 0.5 μm+, unlabeled and LPS labeled 1 μm bead+ *CSF1R*-tg+ and *CSF1R*-tgneg subpopulations 3 h post-IV bead administration analyzed by flow cytometry. Data is shown as the median of 5 or 4 individual animals and error bars indicate 95% confidence intervals. Asterisks indicate statistical significance (*P* < 0.05); **(B)** histological analysis of the location of the beads in the PWP; (i) few 0.5 μm beads were located in *CSF1R*-tg+ Ch68.2+ EAC cells (yellow arrow) whereas *CSF1R*-tg+ Ch68.2neg EAM contain numerous beads (yellow arrow); (ii) the 1 μm beads co-localize with the *CSF1R*-tg+ Ch68.2+ EAC (white arrow) but numerous beads were found in the *CSF1R*-tg+ Ch68.2neg EAM (insert image); (iii) LPS labeled 1 μm beads were located throughout the PWP in *CSF1R*-tg+ MRC1L-Bneg EAC (white arrow) while high concentrations of beads were located in the *CSF1R*-tg+ MRC1L-B+ EAM (yellow arrows). Data is representative of analysis of three individual chickens.

As previously mentioned, cells with the MHCII, MRC1L-Bneg CD11c+ phenotype consist of cDC while MRC1L-B expression is associated with cells of the macrophage lineage (23). Therefore, we used *in vitro* splenic cultures to determine if the low levels of phagocytosis observed in the *CSF1R*-tg+ MRC1L-Bneg cells was due to their location in the spleen rather than a functional aspect of these cells. Firstly, we analyzed the MRC1L-B phenotype of splenocytes grown in the presence of CSF1 by flow cytometry (**Figure 7A**). After 48 h, *CSF1R*-tg+ MRC1L-B+ cells made up around 75% of the total cell population while the *CSF1R*-tg+ MRC1L-Bneg subpopulation made up ∼4% (**Figure 7A** and gating strategy **Supplementary Figure 7A**). We did observe the presence of the *CSF1R*-tgdim MRC1L-B+ subpopulation but not the *CSF1R*-tg− MRC1L-B+ subpopulation in the cultures. As we were interested in analyzing the difference between the MRC1L-B+/neg subpopulations, we focused our analysis on the *CSF1R*-tg+ MRC1L-B+ and MRC1L-Bneg subpopulations. Firstly, cells were treated with unlabeled and LPS-labeled 1 μm beads at 41 or 4°C for 3 h and the phenotype of the bead+ cells followed by the MFI of beads within the subpopulations were analyzed (**Supplementary Figure 7B**). After 3 h, the *CSF1R*-tg+

MRC1L-B+ subpopulation phagocytosed significantly more beads than the *CSF1R*-tg+ MRC1L-Bneg subpopulation, a similar pattern observed *in vivo* (**Figure 7A**). Confocal analysis demonstrated the adherence of both MRC1L-B+ and MRC1L-Bneg subpopulations in the cell cultures (**Figure 7B**i) and the high phagocytic abilities of the MRC1L-B+ cells (**Figure 7B**ii). We also observed the co-localization of MRC1L-B expression with internalized beads indicting its internalization with beads from the cell surface to intracellular vesicles. In addition we observed the co-localization of LAMP1 expression with the phagocytosed beads (**Figure 7B**ii,iii).

We next analyzed whether there was a difference in the ability of the subpopulations to uptake model antigen for transport to intracellular vesicles, such as lysosomes and phagosomes, using *E. coli* and Zymosan bioparticles labeled with the pH-sensitive pHrodo red. As a control, cells were treated with the actin-polymerization inhibitor, Cytochalasin D, 10 min prior to exposure to the bioparticles and the data was normalize by subtracting background fluorescence (**Supplementary Figure 7**). After 3 h, the *CSF1R*-tg+ MRC1L-B+ subpopulation engulfed and transported significantly more bioparticles compared to the *CSF1R*-tg+

FIGURE 7 | *In vitro* functional analysis demonstrates the ability of the *CSF1R*-tg[+] MRC1L-B[neg] cDC to phagocytose model antigens. Splenocytes were culture for 48 h in the presences of CSF1 and phagocytosis was analyzed 3 h post-treatment via flow cytometry. **(A)** After 48 h in culture, *CSF1R*-tg[hi] MRC1L-B[hi] are the dominant subpopulation (75%) compared to the *CSF1R*-tg[dim] MRC1L-B[hi] (12%), *CSF1R*-tg[hi] MRC1L-B[neg] (4%), and *CSF1R*-tg[neg] MRC1L-B[neg] subpopulations (7.5%). MFI of unlabeled and LPS labeled 1 μm beads was significantly higher in the *CSF1R*-tg[+] MRC1L-B[+] subpopulation compared to the *CSF1R*-tg[hi] MRC1L-B[neg] cell population 3 h post-bead treatment; **(B)** confocal analysis demonstrates the (i) adherence of the MRC1L-B[hi] and MRC1L-B^{neg} cells after 48 h in culture; (ii) MRC1L-B^{+} cells phagocytose numerous beads and it expression is localized with internalized beads (white arrows); (iii) intracellular LAMP1 expression co-localizes with
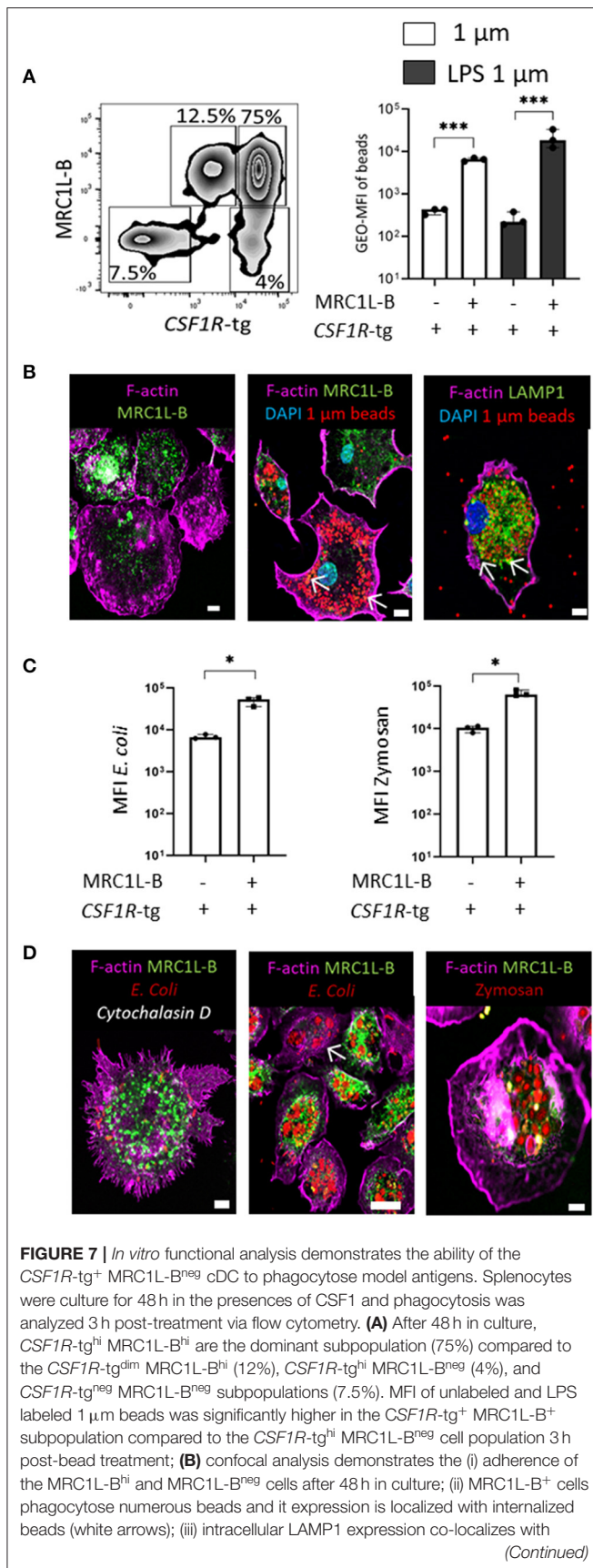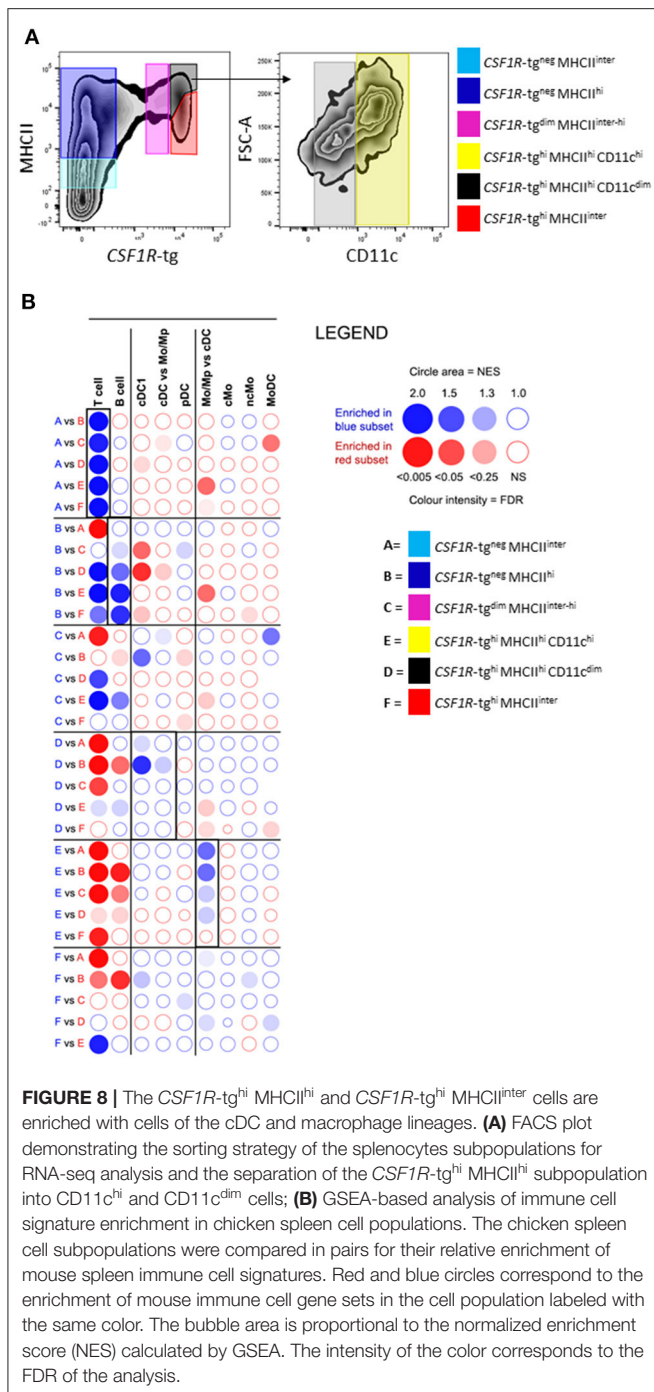
(Continued)

FIGURE 7 | the phagocytosed beads (white arrows); **(C)** MFI of pHrodo red labeled *E. coli* and Zymosan particles demonstrates the ability of the *CSF1R*-tg[hi] MRC1L-B[neg] cDC subpopulation to phagocytose model antigen better than beads suggesting their uptake is more antigen-dependent; **(D)** confocal analysis demonstrates the (i) inhibition of actin polymerization reduces particle uptake but does not affect MRC1L-B expression; (ii, iii) *E. coli* and Zymosan bioparticles are phagocytosed and transported to intracellular vesicles with a high pH environment. Data is shown as the median of 3 individual chickens and error bars indicate 95% confidence intervals. Asterisks indicate statistical significance ($P < 0.05$).

MRC1L-B[neg] subpopulation. However, the data demonstrates the ability of the *CSF1R*-tg[+] MRC1L-B[neg] to phagocytose models antigens better than latex beads and even with their low numbers in the cell culture these cells were highly phagocytic (**Figure 7C**). Microcopy analysis demonstrated the inhibition of actin polymerization prevented the uptake of the bioparticles but it did not affect MRC1L-B expression (**Figure 7D**i–iii). *In vitro* functional analysis demonstrates the ability of the *CSF1R*-tg[+] MRC1L-B[neg] subpopulation to phagocytose model antigen at higher levels than latex beads indicating a more specific pattern of antigen-uptake compared to splenic macrophages.

The *CSF1R*-tg^{hi} MHCII^{hi} CD11c^{hi} and CD11c^{dim} Subpopulations Are Enriched With Cells of the cDC and Macrophage Lineages

We carried out RNA-seq analysis on FACS sorted splenic subpopulations as shown in **Figure 8A**. To determine if the level of putative CD11c expression was specific to a cell subset within the *CSF1R*-tg^{+} subpopulation, we further split the *CSF1R*-tg^{hi} MHCII^{hi} subpopulation into CD11c^{hi} and CD11c^{dim} subpopulations due its lower phenotypical levels of heterogeneity compared to the *CSF1R*-tg^{dim} MHCII[inter−hi] subpopulation (**Figure 8A**). The separation of the *CSF1R*-tg[neg] MRC1L-B[+] subpopulation from the *CSF1R*-tg[neg] MRC1L-B^{neg} cells lead to insufficient cell numbers for their analysis via RNA-seq and therefore these cells were collected with the *CSF1R*-tg[neg] MHCII[hi] subpopulation. Pairwise comparisons of all subpopulations are shown in **Supplementary Table 1**. Using pairwise GSEA, we analyzed whether the transcriptome signatures of murine immune cells were enriched in the sorted splenic subpopulations (23, 54). The *CSF1R*-tg[neg] MHCII[dim] and *CSF1R*-tg[neg] MHCII[hi] subpopulations were significantly enriched for T cell and B cell gene fingerprints compared to the other cell populations (**Figure 8B**). Fingerprints of pDC genes were enriched in the *CSF1R*-tg[neg] MHCII[hi] subpopulation when compared to the *CSF1R*-tg[dim] MHCII[inter−hi] subpopulation but at the lowest level of significance. When comparing the *CSF1R*-tg^{dim} subpopulation, signatures of different cells lineages were enriched, such as T cells, B cells, cDC1, and moDC. The *CSF1R*-tg^{hi} MHCII^{hi} CD11c^{dim} subpopulation was enrichment of fingerprints of cDC1 and cDC vs. Mo/Mp (**Figure 8B**). The *CSF1R*-tg^{hi} MHCII^{hi} CD11c^{hi} subpopulation expressed

FIGURE 8 | The *CSF1R*-tg^{hi} MHCII^{hi} and *CSF1R*-tg^{hi} MHCII[inter] cells are enriched with cells of the cDC and macrophage lineages. **(A)** FACS plot demonstrating the sorting strategy of the splenocytes subpopulations for RNA-seq analysis and the separation of the *CSF1R*-tg^{hi} MHCII^{hi} subpopulation into CD11c^{hi} and CD11c^{dim} cells; **(B)** GSEA-based analysis of immune cell signature enrichment in chicken spleen cell populations. The chicken spleen cell subpopulations were compared in pairs for their relative enrichment of mouse spleen immune cell signatures. Red and blue circles correspond to the enrichment of mouse immune cell gene sets in the cell population labeled with the same color. The bubble area is proportional to the normalized enrichment score (NES) calculated by GSEA. The intensity of the color corresponds to the FDR of the analysis.

Mo/Mp vs. cDC gene signatures. cDC, pDC, Mo/Mp vs. cDC, ncMo, and MoDc gene signatures were enriched in the *CSF1R*-tg[hi] MHCII[inter] subpopulation (**Figure 8B**). The mammalian cDC2 transcriptomic fingerprint could not be established due to the low number of genes to generate reliable statistical analysis. GSEA analysis indicate that the *CSF1R*-tg[hi] MHCII[hi] subpopulation consist of macrophages and cDC.
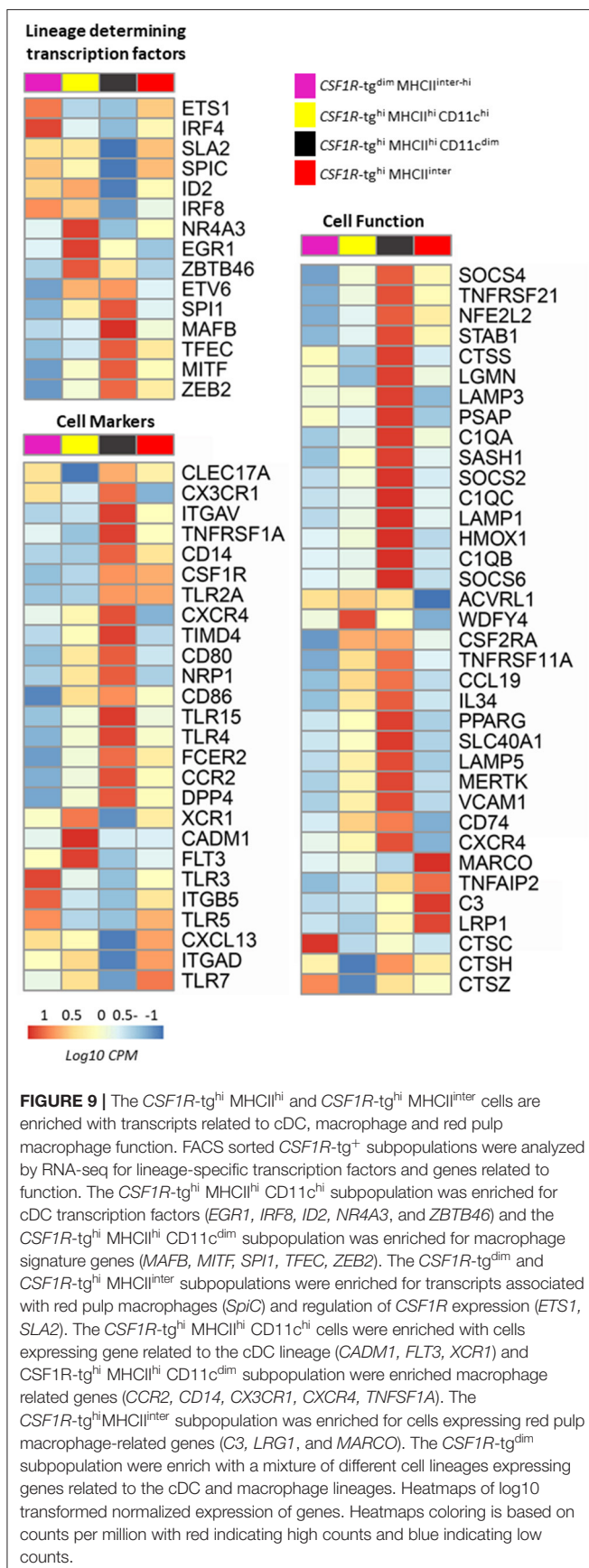
The *CSF1R*-tg[hi] MHCII[hi] and *CSF1R*-tg[hi] MHCII[inter] Subpopulations Express Gene Signatures Characteristic of cDC, Macrophages, and Red Pulp Macrophages

We next analyzed the enrichment of conserved mRNA transcripts characteristic of different cell lineages across the sorted subpopulations. Firstly, core T/NK cell and B cell related genes signatures were analyzed and as expected the *CSF1R*-tg[neg] MHCII[dim] subpopulation were enriched for T/NK cells, significantly expressing *CD3E, CD3D, CD28, CD5, RUNX3,* and *FR2* transcripts whereas the *CSF1R*-tg[neg] MHCII[hi] subpopulation were enriched for B cells, significantly expressing key transcripts such as *CD79B, CXCR5,* and *PAX5* (**Supplementary Figure 8**). The *CSF1R*-tg[dim] MHCII[inter−hi] subpopulation also strongly expressed *CD79B* and *PAX5* (**Supplementary Figure 8**).

Next, the enrichment of cell-fate determining transcriptional regulators involved in macrophage and cDC lineages as reported in the ImmGen Consortium (56) and the mammalian literature were analyzed in the *CSF1R*-tg^{+} subpopulations (**Figure 8B**). The *CSF1R*-tg^{hi} MHCII^{hi} CD11c^{hi} subpopulation was enriched for cells expressing cDC lineage related transcriptional regulators or genes positively associated with cDC differentiation [*EGR1, ID2, IRF8* (56, 57), *NR4A3* (58), and *ZBTB46* (59, 60)] while the *CSF1R*-tg^{hi} MHCII^{hi} CD11c^{dim} subpopulation was enriched for macrophage-related transcription factors [*MAFB* (61, 62), *MITF* (63), *SPI1* (64), *TFEC* (65), and *ZEB2* (66); **Figure 8B**]. The red pulp macrophage-lineage related transcription factor, *SpiC* (67) was expressed at the highest level in the *CSF1R*-tg^{hi} MHCII[inter] subpopulation but also strongly expressed in the *CSF1R*-tg^{hi} MHCII^{hi} CD11c^{hi} and *CSF1R*-tg^{dim} MHCII[inter−hi] subpopulations.

The *CSF1R*-tg^{dim} MHCII[inter−hi] subpopulation expressed higher levels of genes encoding transcripts characteristic of cDC and macrophages (*ETSI, ID2, IRF4, IRF8, SpiC,* and *SLA2*). This observation, along with the expression of B cell and T cell related transcripts, indicates that this subpopulation is very heterogeneous. Overall the *CSF1R*-tg^{hi} MHCII^{hi} CD11c^{hi} and the *CSF1R*-tg^{hi} MHCII^{hi} CD11c^{dim} subpopulations express higher levels of genes characteristic of cDC and macrophage lineages across warm blooded vertebrate species (18, 19, 54). Thus, it can be deduced from this data that the *CSF1R*-tg^{hi} CD11c^{hi} and the *CSF1R*-tg^{hi} CD11c^{dim} subpopulations must primarily encompass cDC and macrophages, respectively.

We next analyzed the enrichment of cell-lineage related surface receptors involved in a number of cellular processes, such as T cell co-stimulation, antigen presentation and migration. cDC related markers *FLT3, CADM1,* and *XCR1* (10, 13), were significantly enriched in the *CSF1R*-tg^{hi} MHCII^{hi} CD11c^{hi} subpopulation whereas macrophage-associated genes, *CSF1R, CD14, CX3CR1, CCR2, CXCR4,* and *TNFSF1A* were enriched in the *CSF1R*-tg^{hi} MHCII^{hi} CD11c^{dim} subpopulation (**Figure 9A**). The *CSF1R*-tg^{hi} MHCII^{hi} CD11c^{dim} subpopulation were enriched for migratory and adhesion related transcripts such as, *CCR7, CDH2, C3AR1,* and *CDH2* (**Supplementary Figure 9**). The integrin *ITGAD* was enriched in the *CSF1R*-tg^{hi} MHCII^{hi} CD11c^{hi} and *CSF1R*-tg^{hi} MHCII[inter] subpopulations whereas

FIGURE 9 | The *CSF1R*-tg^{hi} MHCII^{hi} and *CSF1R*-tg^{hi} MHCII[inter] cells are enriched with transcripts related to cDC, macrophage and red pulp macrophage function. FACS sorted *CSF1R*-tg[+] subpopulations were analyzed by RNA-seq for lineage-specific transcription factors and genes related to function. The *CSF1R*-tg^{hi} MHCII^{hi} CD11c^{hi} subpopulation was enriched for cDC transcription factors (*EGR1, IRF8, ID2, NR4A3,* and *ZBTB46*) and the *CSF1R*-tg^{hi} MHCII^{hi} CD11c^{dim} subpopulation was enriched for macrophage signature genes (*MAFB, MITF, SPI1, TFEC, ZEB2*). The *CSF1R*-tg^{dim} and *CSF1R*-tg^{hi} MHCII[inter] subpopulations were enriched for transcripts associated with red pulp macrophages (*SpiC*) and regulation of *CSF1R* expression (*ETS1, SLA2*). The *CSF1R*-tg^{hi} MHCII^{hi} CD11c^{hi} cells were enriched with cells expressing gene related to the cDC lineage (*CADM1, FLT3, XCR1*) and CSF1R-tg^{hi} MHCII^{hi} CD11c^{dim} subpopulation were enriched macrophage related genes (*CCR2, CD14, CX3CR1, CXCR4, TNFSF1A*). The *CSF1R*-tg^{hi}MHCII[inter] subpopulation was enriched for cells expressing red pulp macrophage-related genes (*C3, LRG1,* and *MARCO*). The *CSF1R*-tg[dim] subpopulation were enrich with a mixture of different cell lineages expressing genes related to the cDC and macrophage lineages. Heatmaps of log10 transformed normalized expression of genes. Heatmaps coloring is based on counts per million with red indicating high counts and blue indicating low counts.

ITGAV transcript was enriched in *CSF1R*-tg^{hi} MHCII^{hi} CD11c^{dim} subpopulation. Co-stimulatory molecules, *CD80* and *CD86* transcripts were significantly expressed by cells within the *CSF1R*-tg^{hi} MHCII^{hi} CD11c^{hi} and CD11c^{dim} subpopulations. *DPP4* (CD26) is highly expressed in the *CSF1R*-tg^{hi} MHCII^{hi} CD11c^{dim} subpopulation (not CD11c^{hi}), which is not consistent with DPP4 being expressed to high levels selectively on cDC1 in humans, mice, and sheep (19). We next analyzed the expression of Toll-like receptors (TLR) transcripts across the *CSF1R*-tg^{+} subpopulations and found that the *CSF1R*-tg^{hi} MHCII^{hi} CD11c^{dim} subpopulation was enriched for cells expressing *TLR4, TLR2A* and co-receptor, *CD14*. The *CSF1R*-tg^{hi} MHCII[inter] subpopulation expressed high levels of C-type lectin receptors, *FCER2* (CLEC17AL-A), and *CLEC17A* (CLEC17AL-B) (68). The apoptotic cell recognition receptor, *TIMD4* (69) transcript expression was enriched in both the *CSF1R*-tg^{hi} MHCII^{hi} CD11c^{hi} and CD11c^{dim} subpopulations (**Figure 9A**).

The *CSF1R*-tg^{hi} MHCII^{hi} CD11c^{hi} subpopulation significantly expressed genes involved in cross-presentation and MHCII-associated genes [*ACVRL1* (70), *CD74, LAMP5* (71), and *WDFY4* (72)]. Key macrophage related genes, *MERTK, VCAM1,* and genes related to red pulp and alternatively activated macrophages, *C1QA, C1QB,* and *PPARG* (73), and suppressor of cytokine signaling molecules (*SOCS2, SOCS4,* and *SOCS6*) were highly expressed in the *CSF1R*-tg^{hi} MHCII^{hi} CD11c^{dim} subpopulation compared to the CD11c^{hi} subpopulation. An array of transcripts involved in antigen processing [*CD74, CTSS, LGMN, LAMP1, LAMP3, LAMP5, MERTK,* and *PSAP* (71)] were also strongly expressed by the *CSF1R*-tg^{hi} MHCII^{hi} CD11c^{dim} subpopulation (**Figure 9B**). The *CSF1R*-tg^{hi} MHCII[inter] subpopulation expressed the highest levels of genes characteristic of the red pulp macrophage lineage, *MARCO, C3,* and *LRG1* (73). Chicken heterophils express the *CSF1R*-tg at low levels (33, 34). Therefore, we analyzed the expression of core heterophil gene transcripts across the *CSF1R*-tg[+] subpopulations (74) and found no significant enrichment of heterophil related gene transcripts in any of the *CSF1R*-tg[+] subpopulations (**Supplementary Table 2**). The *CSF1R*-tg[dim] MHCII[inter−hi] subpopulation were enriched for cathepsins family members (*CTSC, CTSH,* and *CTSZ*) but no clear definition of what enriched macrophage cell type this subpopulation represented was identified. To analyze whether the *CSF1R*-tg[dim] subpopulation were true phagocytic cells and not an artifact of transgene expression or cells undergoing physiological stress, we carried out an *in vivo* liposome depletion study, where phagocytic cells were targeted for depletion by apoptosis induction after the uptake of clondronate liposomes (75). Three days after a single IV-administration of liposomes, we observed a severe depletion of the *CSF1R*-tg[dim] MRC1L-B[+] subpopulation in chickens treated with the clondronate liposomes compared to those treated with PBS liposomes indicating that this subpopulation contains phagocytic cells belonging to the MPS (**Supplementary Figure 10**). Although our sorting approach would not have led to pure cell populations, we were able to determine the enrichment of cDC in the *CSF1R*-tg^{hi} MHCII^{hi} CD11c^{hi} subpopulations as previously described (23). Furthermore, we demonstrated the existence of at least

three subsets of resident tissue macrophages in the chicken spleen. Based on the RNA-seq and immunohistological analysis, the *CSF1R*-tg^{hi} MHCII^{hi} CD11c^{low} subpopulation are enriched with macrophages from the PWP and PALS while the *CSF1R*-tg^{hi} MHCII[inter] cells are enriched with red pulp macrophages. Although we cannot demonstrate which splenic cell they represent, the *CSF1R*-tg[dim] MHCII[inter−hi] MRC1L-B[+] are a subset of the chicken splenic MPS.

DISCUSSION

Mononuclear phagocytes reside within distinct niches of the spleen where they partake in the number of cellular processes from homeostasis, removal of aged, or damaged erythrocytes to killing of pathogens and induction of adaptive immune responses. The development, proliferation, and survival of monocytes, macrophages, and cDC are controlled by CSF1R [reviewed by (76)]. Lineage specific expression of CSF1R has allowed for the detailed study of the MPS using the *CSF1R*-reporter transgenic chickens. Since their generation, transcriptome analysis of bursal macrophages, liver macrophages, and to some extent cDC, along with subsets of blood monocytes have been described (22). Hu et al., observed the lack of *CSF1R*-tg expression in chicken Kupffer cells that express similar CSF1R mRNA levels as tissue macrophages. In certain cell types in mice, CSF1R expression is under controlled of a 150 bp distal promoter not included in the generation of the *CSF1R*-reporter chickens and thus is inferred as the reason for the lack of *CSF1R*-tg expression in chicken Kupffer cells (22, 77). The splenic MPS cells has been described based on their MHCII, MRC1L-B, Ch74.2 expression, and acid-phosphatase staining and to a certain extent using the *CSF1R*-reporter transgenic chickens (24, 25, 29, 33, 78–80). However, the separation of PALS and PWP macrophages has not been described while comparative gene profiling has identified the existence of the XCR1 cDC in the chicken spleen but not their location (23). Using the *CSF1R*-reporter transgenic chickens we carried out a comprehensive analysis of the splenic MPS.

In the chicken spleen, interdigitating cells (also known as interdigitating DC) and PALS-associated macrophages express MHCII and MRC1L-B while MHCII^{hi} CD11c^{+} MRC1L-B^{neg} cells are enriched for cDC (28, 29). As the CD11c, 8F2 antibody is not commercially available, progress in the field of chicken DC research has been limited. Using the *CSF1R*-reporter transgenic chickens, we observed a *CSF1R*-tg[+] subpopulation lacking MRC1L-B expression in the PALS (**Figure 1**) demonstrating that these chicken models can be used to study cDC without requiring specific cDC antibodies such as FLT3. In the PWP, the equivalent of the mammalian MZ, two subpopulations have previously been shown to express the *CSF1R*-tg (22, 33). On the outer margins of the PWP, intermingled with B cells are the *CSF1R*-tg[+] EAM while the *CSF1R*-tg[+] EAC are anchored into the ellipsoid (81). In contrast to EAM, EAC lack MRC1L-B and MHCII expression and specifically stain for Ch68.2, a chicken monoclonal which binds to an unknown epitope (25, 28). In this study, we show that EAC express higher levels of CD11c compared to the EAM

[**Figure 1**; (23, 42)]. Due to their location in the PWP, the EAM resemble the mammalian MZM which function to trap and display antibody-coated antigens from the blood for transfer to the MZ B cells which is subsequently deposit to FDC in the follicles (82). However, in chickens, surface antigen display has been observed in EAC but not EAM (28, 83). The high level of CD11c expression by the EAC may correlate with their ability to detach from the ellipsoid upon antigen exposure and their subsequent migration to the PALS to develop into FDC (28). We found intracellular punctate expression of MHCII by EAC but could not fully determine whether these cells express surface MHCII (**Figure 2**). These cells were found to express LAMP1, possibly demonstrating their ability to digest substances delivered by endocytosis and phagocytosis (84). In the red pulp, we found that the *CSF1R*-tg^{+} cells express high levels of MRC1L-B but not all stained for the chicken macrophage marker, Ch74.2 as previously described (24). A previous study has described the presence of CD45^{+} Ch68.2^{neg} cells within the inner regions of the ellipsoid (28). We observed cells lacking *CSF1R*-tg expression in a similar location in the ellipsoid and found they express high levels of MHCII, MRC1L-B, CD11c, LAMP1, and CSF1R (22). We have called this cell population "ellipsoid macrophages" (EM). The EM may represent incoming monocytes or ellipsoid resident macrophages and requires further study in the future. Through flow cytometry we show that *CSF1R*-tg[neg] MRC1L-B^{+} cells express high levels of CD80, CD40, and the chicken monocyte/thrombocyte marker, K1 (**Supplementary Figure 4**).

When analyzing the phenotype of cells via flow cytometry we found that splenic MPS diversely express the *CSF1R*-tg and MHCII. One subpopulation could be distinguished based on their *CSF1R*-tg[dim] MHCII[inter−hi] phenotype while two subpopulations expressed similar levels of the *CSF1R*-tg and were separated based on MHCII[hi] and MHCII[inter] levels (**Figure 3**). We found that the *CSF1R*-tg[dim] and *CSF1R*-tg[hi] MHCII[hi] subpopulations were very heterogenic in their MRC1L-B and CD11c expression levels while the *CSF1R*-tg[hi] MHCII[inter] subpopulation expressed these markers more uniformly (**Figure 3**). We did not identify a cell phenotype resembling EAC or FDC which have the *CSF1R*-tg^{+} MHCII[neg/low] MRC1L-B^{neg} CD11c^{+} phenotype (28, 33). This may be due to their lack of survival during cell isolation or they express low or dynamic levels of MHCII. Although there is an EAC-specific surface marker, Ch68.2, this antibody fails to provide consistent staining in flow cytometry (data not shown). Further phenotypical analysis demonstrated low expression levels of CD80, CD40, MHCI, and CD44 in the *CSF1R*-tg[hi] MHCII[inter] subpopulation compared to the *CSF1R*-tg[dim] and *CSF1R*-tg[hi] MHCII[hi] subpopulations (**Figure 4**). The *CSF1R*-tg[hi] MHCII[inter] subpopulation express low levels of Ch74.2 which was also observed for red pulp macrophages via immunohistology (**Figure 4**). Mammalian red pulp macrophages express low level of co-stimulatory molecules and MHCII due to their reduced role in T cell antigen presentation (2). These observations would suggest that the *CSF1R*-tg[hi] MHCII[inter] subpopulation may consist of red pulp macrophages.

In vivo functional analysis demonstrated that the *CSF1R*-tg[hi] MHCII[hi] subpopulation phagocytosed significantly more

beads compared to the *CSF1R*-tg^{dim} and *CSF1R*-tg^{hi} MHCII^{inter} subpopulations while labeling beads with LPS increased the phagocytosis of the *CSF1R*-tg^{hi} MHCII^{inter} subpopulation (**Figure 5**). LPS has been shown to enhance antigen uptake by chicken red pulp macrophages (24). In a recent study, *ex vivo* isolated splenic MRC1L-B^{hi} MHCII^{lo} cells showed higher phagocytosis of dead cells than MRC1L-B^{lo} MHCII^{hi} cells with the latter cell population suggested to represent red pulp macrophages. Another study has also demonstrated the expression of the apoptotic cell receptor, Tim4, by EAM which we show express high levels of MRC1L-B [**Figure 1**; (22, 85)]. Therefore, the previous characterized, MRC1L-B^{hi} MHCII^{lo} cells may represent a heterogeneous population of red pulp macrophages and EAM. *In vivo* functional analysis indicated that the majority of the bead^{+} *CSF1R*-tg^{+} subpopulations expressed MRC1L-B. When we analyzed location of the beads in the spleen we observed large deposits in the EAM while few beads were observed associated with EAC (**Figure 6**). Both flow cytometric and immunohistological analysis suggests that a subsets of *CSF1R*-tg^{dim} MHCII$^{inter-hi}$ MRC1L-B^{+} and *CSF1R*-tg^{hi} MHCII^{hi} MRC1L-B^{+} subpopulations are located in the PWP demonstrating that EAM differ in their *CSF1R*-tg expression levels but not MRC1L-B. For the bead^{+} *CSF1R*-tg^{hi} MHCII^{inter} subpopulation, we speculate that these cells are either a subset of EAM or red pulp macrophages residing in close proximity to the EAM, hence their ability to capture antigens.

We observed very little *in vivo* bead uptake by the *CSF1R*-tg^{+} MHCII^{+} MRC1L-B^{neg} cells which may be due to their higher numbers in the PALS and not the PWP where antigen capture primarily takes place. *In vitro* functional analysis demonstrated that the *CSF1R*-tg^{+} MRC1L-B^{neg} subpopulation were capable of phagocytosis (**Figure 7**). Mammalian macrophages express large intracellular pools of MRC1 within their early endosomes, which undergo continual rapid recycling to the cell surface to endocytose bound antigens (86). Due the high recycling nature of MRC1 in mammals and the fixture of adherent cells with PFA in this study, we only observed intracellular punctate expression of MRC1L-B (**Figure 7**). However, we found the co-localization of MRC1L-B and LAMP1 expression with the internalized beads *in vitro* which for the first time demonstrates the ability of MRC1L-B to traffic with antigens to lysosomes and endosomes similar to mammalian MRC1 (86). Our *in vivo* functional analysis provided the first demonstration of antigen uptake by the *CSF1R*-tg^{+} MRC1L-B^{neg} cDC subpopulation in the spleen further demonstrating the ability to study cDC *ex vivo* using the *CSF1R*-transgenic chickens. In addition, future studies using the *CSF1R*-transgenic chickens and pathogens would allow for the *in vivo* visualization of cDC-T cell interactions in the chicken spleen.

Transcriptomic analysis has shown the conservation of MPS lineage specific gene signatures throughout distantly related mammals (18, 19, 23, 54). A previous comparative analysis of chicken splenic cells demonstrated the existence of cDC which expressed the MHCII^{+} MRC1L-B^{neg} CD11c^{+} phenotype by their enrichment for XCR1, FLT3, and key cDC lineage gene transcripts. The authors also described the enrichment of macrophage related genes in MRC1L-B^{+} cells (23). We expanded on this study by separating the *CSF1R*-tg^{hi} MHCII^{hi}

subpopulation into CD11c^{hi} and CD11c^{dim} subsets and analyzing two additional subsets of splenic MPS via RNA-seq analysis (**Figure 8**). It should be noted that MRC1-B^{+} cells were not excluded from the *CSF1R*-tg^{+} subpopulations as performed in the Vu Manh et al., study (23). Primarily we analyzed the presence of murine splenic immune cell gene signatures using GSEA across all the cell subpopulations (**Figure 8**). We initially found an enrichment of the cDC1 gene signatures in the *CSF1R*-tg^{hi} MHCII^{hi} CD11c^{hi} subpopulation and macrophage gene signatures in the *CSF1R*-tg^{hi} MHCII^{hi} CD11c^{dim} subpopulation. We found that the *CSF1R*-tg^{dim}MHCII$^{inter-hi}$ subpopulations contained cells expressing B cell, T cell, cDC, and macrophage gene signatures which correlates with the immuno-phenotyping analysis (**Figures 3**, **4**). Upon closer analysis of the enrichment of genes associated with cell lineage development and function, we found that the *CSF1R*-tg^{hi} MHCII^{hi} CD11c^{hi} subpopulation were enriched for genes characteristic of the cDC lineage (*IRF8, ID2, ZEB2, FLT3, XCR1*, and *CAMD1*) although they contain ~30% of MRC1L-B^{neg-hi} cells which may suggest that a significant fraction of chicken cDC express MRC1L-B contrary what was previously reported or this population contains non-cDCs that express MRC1L-B (23). This subpopulation contained cells enriched for genes also involved in cross-presentation and MHCII processing [*WDFY4, ACVRL1, CD74*, and *LAMP5*; (72)]. However, in contrast to human, mouse, and sheep cDC, we found strong expression of DPP4 in chicken cells corresponding to macrophages, *CSF1R*-tg^{hi} MHCII^{hi} CD11c^{dim} cells, discussed later, and not chicken cDC (19, 87). This suggests that chicken macrophages may have a role in T cell-stimulation (88). The hallmark of cDC is their ability to present to and activate T cells, however, numerous attempts to demonstrate DC-T cell interaction through MLR were to no avail, with numerous cells of the MPS engulfing/phagocytosing labeled CD4^{+} T cells (data not shown).

The *CSF1R*-tg^{hi} MHCII^{hi} CD11c^{dim} subpopulation were enriched for genes characteristic of macrophages [*CCR2, CD14, CD36, CSF1R, CXCR4, CX3CR1, HIF1A, MAFB, MITF, STAT1, SPI1, TLR4*, and *TNFSF1A*; (22, 76)]. This subpopulation was also enriched for M2 anti-inflammatory cell phenotype and red pulp macrophage related gene transcripts (*C1QA C1QB*, and *PPARG*) which are associated with tissue repair and homeostasis (89). Based on their CD11c^{dim} phenotype these macrophages likely represent the EAM and PAL-associated macrophages in the spleen. Distinguishing the difference between the EAM and PAL-associated macrophages requires further investigation. The *CSF1R*-tg^{hi} MHCII^{inter} subpopulation was enriched for genes associated with red pulp macrophages [*HEPHL1, LRP1, SpiC*, and *TF*; (67)]. Similar to the *CSF1R*-tg^{hi} MHCII^{hi} subpopulation, we cannot rule out the possibility of the *CSF1R*-tg^{hi} MHCII^{inter} subpopulation containing more than one macrophage cell lineage, such as PALS-associated macrophages. The *CSF1R*-tg^{dim} subpopulation were phenotypically heterogeneous and may represent cells undergoing different levels of development or activation in the spleen and require further analysis. In the murine spleen, pDC make up around 0.5% of cells (90). In our analysis, we found low levels of pDC gene signatures in the *CSF1R*-tg^{neg} MHCII^{hi} subpopulation which may be

TABLE 2 | An overview of the phenotype and phagocytosis abilities of MPS in the chicken spleen as determined by immunohistology and flow cytometry.

	Phenotype								*In vivo* phagocytosis	
CSF1R-tg	MHCII	MRC1L-B	CD11c	CD80	CD40	MHCI	ChB6	Ch74.2	MRC1L-B positive	MRC1L-B negative
Negative	Hi	Hi	Hi	Hi	Hi	N/D	–	N/D	++	N/D
Dim	Inter	Neg/Low	Hi	Hi	Hi	Hi	+/–	Hi	+++	+
	Hi	Inter	Inter-Hi							
		Hi	Hi							
High	Hi	Neg/Low	Hi	Hi	Hi	Hi	–	Hi	++++	+
		Inter	Inter							
		Hi	Hi							
High	Inter	Neg/Low	Hi	Low	Low	Low	–	Low	+++	+
		Hi	Hi							

The level of surface marker expression in the CSF1R-tg⁺ and CSF1R-tgⁿᵉᵍ subpopulations are indicated as negative to low (Neg), intermediate (Inter), and high (Hi). N/D, not determined. The + symbols indicate the level of phagocytosis in the CSF1R-tg⁺ MRC1L-B⁺ or MRC1L-Bⁿᵉᵍ cells.

related to the MRC1L-B$^+$ cells present in this subpopulation (**Figure 3E**). However, more analysis is required to confirm the existence of this cell lineage in chickens. As of yet, no definitive study has identified different chicken cDC subsets as observed in mammals possible indicating the existence of just one cDC subset in chickens. We did observed the cDC2 related transcription factor, IRF4, in the *CSF1R*-tg^{dim} subpopulation but this may be due to the mixture of B cell, cDC, and macrophage lineages in this subset (91–93). Future single cell RNA-seq analysis of splenocytes has the potential to further contribute to delineating the cells of the chicken splenic MPS.

In conclusion, we have shown that the *CSF1R*-reporter transgenic chickens can be used to distinguish different cell subsets of the MPS in the spleen. We have demonstrated that the PALS-associated *CSF1R*-tg$^+$ cells do not uniformly express MRC1L-B helping to differentiate PALS-associated cDC (MRC1L-B^{neg}) from macrophages (MRC1L-B$^+$) in the chicken spleen. In the PWP, a novel *CSF1R*-tg^{neg} cell population, called ellipsoid macrophages were also characterized. We demonstrated that there are at least three distinctive cell subpopulations expressing diverse levels of *CSF1R*-tg and MHCII in the chicken spleen. In addition, we demonstrated that the *CSF1R*-tg^{hi} MHCII^{inter} subpopulation, phenotypically, and functionally resemble red pulp macrophages and identified functional diversity in EAM. For the first time we demonstrated the functionality of *CSF1R*-tg$^+$ MRC1L-B^{neg} cDC *in vitro*. The phenotype and function of chicken splenic MPS are provided as an overview in **Table 2**. This is the first description of the function and transcriptome of a number of MPS cell lineages in chicken spleen that will contribute to future studies to dissect their roles in antigen presentation, immune responses, and resolve the EAC and FDC cell lineages and functions.

DATA AVAILABILITY STATEMENT

The datasets presented in this study can be found in online repositories. The names of the repository/repositories and accession number(s) can be found in the article/**Materials and Methods**.

ETHICS STATEMENT

The animal study was conducted under Home Office project license PE263A4FA according to the requirements of the Animal (Scientific Procedures) Act 1986, with the approval of the Roslin Institute's ethical review committees. Birds were humanely culled in accordance with Schedule 1 of the Animals (Scientific Procedures) Act 1986.

AUTHOR CONTRIBUTIONS

KS, LV, and AB conceptualized the study. KS, DB, and LV performed or assisted with the bird experiments. KM performed the transcriptomic data analysis. KS performed all experiments and analysis. LV, PK, and HS secured the funding. KS wrote the manuscript. All authors contributed to read and approved the final manuscript.

FUNDING

ACKNOWLEDGMENTS

initial analysis) was carried out by Edinburgh Genomics at the University of Edinburgh.

SUPPLEMENTARY MATERIAL

The Supplementary Material for this article can be found online at: https://www.frontiersin.org/articles/10.3389/fimmu.2021.636436/full#supplementary-material

Supplementary Figure 1 | The dynamic expression of CD11c and MHCII in the chicken spleen.

Supplementary Figure 2 | Multicolor confocal analysis of the PWP.

Supplementary Figure 3 | Gating strategy for flow cytometric analysis and FACS.

Supplementary Figure 4 | Immuno-phenotyping of the *CSF1R*-tg+ and *CSF1R*-tg− cells in the chicken spleen.

Supplementary Figure 5 | Phenotypical analysis of the *CSF1R*-tg^neg MRC1L-B+ cells in the chicken spleen and thrombocyte cell analysis.

Supplementary Figure 6 | Analysis of the location of fluorescent bead particles 3 h post-IV administration in chicken spleen.

Supplementary Figure 7 | Flow cytometric analysis of adherent primary chicken splenocytes cultured for 48 h and *in vitro* phagocytosis controls at 4°C and Cytochalasin D treatment.

Supplementary Figure 8 | RNA-seq analysis of the chicken splenic subpopulations indicate enrichment for core T cell, NK cell, and B cell in the *CSF1R*-tg^neg subpopulations.

Supplementary Figure 9 | RNA-seq analysis of the chicken *CSF1R*-tg+ subpopulations indicate enrichment of migratory and adhesion related genes in the *CSF1R*-tg^hi MHCII^hi CD11c^dim subpopulations.

Supplementary Figure 10 | The *CSF1R*-tg^dim subpopulations are depleted 3 days post-clondronate liposome treatment.

Supplementary Table 1 | Differentially expressed genes comparison in splenic *CSF1R*-tg^neg and *CSF1R*-tg+ subpopulations (FDR <0.5).

Supplementary Table 2 | Differentially expressed chicken heterophil related genes comparison in splenic *CSF1R*-tg+ subpopulations (FDR <0.5).

REFERENCES

1. Guilliams M, Ginhoux F, Jakubzick C, Naik SH, Onai N, Schraml BU, et al. Dendritic cells, monocytes and macrophages: a unified nomenclature based on ontogeny. *Nat Rev Immunol.* (2014) 14:571–8. doi: 10.1038/nri3712

2. Kurotaki D, Kon S, Bae K, Ito K, Matsui Y, Nakayama Y, et al. CSF-1-dependent red pulp macrophages regulate CD4 T cell responses. *J Immunol.* (2011) 186:2229–37. doi: 10.4049/jimmunol.1001345

3. Kurotaki D, Uede T, Tamura T. Functions and development of red pulp macrophages. *Microbiol Immunol.* (2015) 59:55–62. doi: 10.1111/1348-0421.12228

4. Swirski FK, Nahrendorf M, Etzrodt M, Wildgruber M, Cortez-Retamozo V, Panizzi P, et al. Identification of splenic reservoir monocytes and their deployment to inflammatory sites. *Science.* (2009) 325:612–6. doi: 10.1126/science.1175202

5. Kim E, Yang J, Beltran CD, Cho S. Role of spleen-derived monocytes/macrophages in acute ischemic brain injury. *J Cereb Blood Flow Metab.* (2014) 34:1411–9. doi: 10.1038/jcbfm.2014.101

6. Steiniger BS. Human spleen microanatomy: why mice do not suffice. *Immunology.* (2015) 145:334–46. doi: 10.1111/imm.12469

7. Mebius RE, Kraal G. Structure and function of the spleen. *Nat Rev Immunol.* (2005) 5:606–16. doi: 10.1038/nri1669

8. Ito S, Naito M, Kobayashi Y, Takatsuka H, Jiang S, Usuda H, et al. Roles of a macrophage receptor with collagenous structure (MARCO) in host defense and heterogeneity of splenic marginal zone macrophages. *Arch Histol Cytol.* (1999) 62:83–95. doi: 10.1679/aohc.62.83

9. Aichele P, Zinke J, Grode L, Schwendener RA, Kaufmann SH, Seiler P. Macrophages of the splenic marginal zone are essential for trapping of blood-borne particulate antigen but dispensable for induction of specific T cell responses. *J Immunol.* (2003) 171:1148–55. doi: 10.4049/jimmunol.171.3.1148

10. Sichien D, Scott CL, Martens L, Vanderkerken M, Van Gassen S, Plantinga M, et al. IRF8 transcription factor controls survival and function of terminally differentiated conventional and plasmacytoid dendritic cells, respectively. *Immunity.* (2016) 45:626–40. doi: 10.1016/j.immuni.2016.08.013

11. Bachem A, Hartung E, Güttler S, Mora A, Zhou X, Hegemann A, et al. Expression of XCR1 characterizes the Batf3-dependent lineage of dendritic cells capable of antigen cross-presentation. *Front Immunol.* (2012) 3:214. doi: 10.3389/fimmu.2012.00214

12. Edelson BT, KC W, Juang R, Kohyama M, Benoit LA, Klekotka PA, et al. Peripheral CD103+ dendritic cells form a unified subset developmentally related to CD8α+ conventional dendritic cells. *J Exp Med.* (2010) 207:823–36. doi: 10.1084/jem.20091627

13. Dorner BG, Dorner MB, Zhou X, Opitz C, Mora A, Guttler S, et al. Selective expression of the chemokine receptor XCR1 on cross-presenting dendritic cells determines cooperation with CD8+ T cells. *Immunity.* (2009) 31:823–33. doi: 10.1016/j.immuni.2009.08.027

14. Schlitzer A, McGovern N, Teo P, Zelante T, Atarashi K, Low D, et al. IRF4 transcription factor-dependent CD11b+ dendritic cells in human and mouse control mucosal IL-17 cytokine responses. *Immunity.* (2013) 38:970–83. doi: 10.1016/j.immuni.2013.04.011

15. Ghosh HS, Cisse B, Bunin A, Lewis KL, Reizis B. Continuous expression of the transcription factor e2-2 maintains the cell fate of mature plasmacytoid dendritic cells. *Immunity.* (2010) 33:905–16. doi: 10.1016/j.immuni.2010.11.023

16. Cisse B, Caton ML, Lehner M, Maeda T, Scheu S, Locksley R, et al. Transcription factor E2-2 is an essential and specific regulator of plasmacytoid dendritic cell development. *Cell.* (2008) 135:37–48. doi: 10.1016/j.cell.2008.09.016

17. Schlitzer A, Ginhoux F. Organization of the mouse and human DC network. *Curr Opin Immunol.* (2014) 26:90–9. doi: 10.1016/j.coi.2013.11.002

18. Vu Manh TP, Bertho N, Hosmalin A, Schwartz-Cornil I, Dalod M. Investigating evolutionary conservation of dendritic cell subset identity and functions. *Front Immunol.* (2015) 6:260. doi: 10.3389/fimmu.2015.00260

19. Contreras V, Urien C, Guiton R, Alexandre Y, Vu Manh TP, Andrieu T, et al. Existence of CD8alpha-like dendritic cells with a conserved functional specialization and a common molecular signature in distant mammalian species. *J Immunol.* (2010) 185:3313–25. doi: 10.4049/jimmunol.1000824

20. Park KT, ElNaggar MM, Abdellrazeq GS, Bannantine JP, Mack V, Fry LM, et al. Phenotype and function of CD209+ bovine blood dendritic cells, monocyte-derived-dendritic cells and monocyte-derived macrophages. *PLoS ONE.* (2016) 11:e0165247. doi: 10.1371/journal.pone.0165247

21. Summerfield A, Auray G, Ricklin M. Comparative dendritic cell biology of veterinary mammals. *Annu Rev Anim Biosci.* (2015) 3:533–57. doi: 10.1146/annurev-animal-022114-111009

22. Hu T, Wu Z, Bush SJ, Freem L, Vervelde L, Summers KM, et al. Characterization of subpopulations of chicken mononuclear phagocytes that express TIM4 and CSF1R. *J Immunol.* (2019) 202:1186–99. doi: 10.4049/jimmunol.1800504

23. Vu Manh TP, Marty H, Sibille P, Le Vern Y, Kaspers B, Dalod M, et al. Existence of conventional dendritic cells in *Gallus gallus* revealed by comparative gene expression profiling. *J Immunol.* (2014) 192:4510–7. doi: 10.4049/jimmunol.1303405

24. Jeurissen SH, Claassen E, Janse EM. Histological and functional differentiation of non-lymphoid cells in the chicken spleen. *Immunology.* (1992) 77:75–80.

25. Jeurissen SH, Janse EM, Kok GL, De Boer GF. Distribution and function of non-lymphoid cells positive for monoclonal antibody CVI-ChNL-68.2 in healthy chickens and those infected with Marek's disease virus. *Vet Immunol Immunopathol.* (1989) 22:123–33. doi: 10.1016/0165-2427(89)90055-x

26. Jeurissen SHM, Janse EM, Koch G, de Boer GF. The monoclonal antibody CVI-CHNL-68.1 recognizes cells of the monocyte-macrophage lineage in chickens. *Dev Comp Immunol.* (1988) 12:855–64. doi: 10.1016/0145-305X(88)90059-6

27. Oláh I, Glick B. Splenic white pulp and associated vascular channels in chicken spleen. *Am J Anat.* (1982) 165:445–80. doi: 10.1002/aja.1001650408

28. Igyártó BZ, Magyar A, Oláh I. Origin of follicular dendritic cell in the chicken spleen. *Cell Tissue Res.* (2007) 327:83–92. doi: 10.1007/s00441-006-0250-0

29. Mast J, Goddeeris BM, Peeters K, Vandesande F, Berghman LR. Characterisation of chicken monocytes, macrophages and interdigitating cells by the monoclonal antibody KUL01. *Vet Immunol Immunopathol.* (1998) 61:343–57. doi: 10.1016/s0165-2427(97)00152-9

30. Staines K, Hunt LG, Young JR, Butter C. Evolution of an expanded mannose receptor gene family. *PLoS ONE.* (2014) 9:e110330. doi: 10.1371/journal.pone.0110330

31. Dai XM, Ryan GR, Hapel AJ, Dominguez MG, Russell RG, Kapp S, et al. Targeted disruption of the mouse colony-stimulating factor 1 receptor gene results in osteopetrosis, mononuclear phagocyte deficiency, increased primitive progenitor cell frequencies, and reproductive defects. *Blood.* (2002) 99:111–20. doi: 10.1182/blood.v99.1.111

32. Karsunky H, Merad M, Cozzio A, Weissman IL, Manz MG. Flt3 ligand regulates dendritic cell development from Flt3+ lymphoid and myeloid-committed progenitors to Flt3+ dendritic cells *in vivo. J Exp Med.* (2003) 198:305–13. doi: 10.1084/jem.20030323

33. Balic A, Garcia-Morales C, Vervelde L, Gilhooley H, Sherman A, Garceau V, et al. Visualisation of chicken macrophages using transgenic reporter genes: insights into the development of the avian macrophage lineage. *Development.* (2014) 141:3255–65. doi: 10.1242/dev.105593

34. Alber A, Morris KM, Bryson KJ, Sutton KM, Monson MS, Chintoan-Uta C, et al. Avian Pathogenic *Escherichia coli* (APEC) strain-dependent immunomodulation of respiratory granulocytes and mononuclear phagocytes in CSF1R-reporter transgenic chickens. *Front. Immunol.* (2020) 10:3055. doi: 10.3389/fimmu.2019.03055

35. Garceau V, Balic A, Garcia-Morales C, Sauter KA, McGrew MJ, Smith J, et al. The development and maintenance of the mononuclear phagocyte system of the chick is controlled by signals from the macrophage colony-stimulating factor receptor. *BMC Biol.* (2015) 13:12. doi: 10.1186/s12915-015-0121-9

36. Sutton K, Costa T, Alber A, Bryson K, Borowska D, Balic A, et al. Visualisation and characterisation of mononuclear phagocytes in the chicken respiratory tract using CSF1R-transgenic chickens. *Vet Res.* (2018) 49:104. doi: 10.1186/s13567-018-0598-7

37. Kaufman J, Skjoedt K, Salomonsen J, Simonsen M, Du Pasquier L, Parisot R, et al. MHC-like molecules in some nonmammalian vertebrates can be detected by some cross-reactive xenoantisera. *J Immunol.* (1990) 144:2258–72.

38. Guillemot FP, Oliver PD, Peault BM, Le Douarin NM. Cells expressing Ia antigens in the avian thymus. *J Exp Med.* (1984) 160:1803–19. doi: 10.1084/jem.160.6.1803

39. Salomonsen J, Skjodt K, Crone M, Simonsen M. The chicken erythrocyte-specific MHC antigen. Characterization and purification of the B-G antigen by monoclonal antibodies. *Immunogenetics.* (1987) 25:373–82. doi: 10.1007/BF00396103

40. Salomonsen J, Sørensen MR, Marston DA, Rogers SL, Collen T, van Hateren A, et al. Two CD1 genes map to the chicken MHC, indicating that CD1 genes are ancient and likely to have been present in the primordial MHC. *Proc Natl Acad Sci USA.* (2005) 102, 8668–73. doi: 10.1073/pnas.0409213102

41. Ly N, Danzl NM, Wang J, Zajonc DM, Dascher CC. Conservation of CD1 protein expression patterns in the chicken. *Dev Comp Immunol.* (2010) 34:123–32. doi: 10.1016/j.dci.2009.08.015

42. Wu Z, Rothwell L, Young JR, Kaufman J, Butter C, Kaiser P. Generation and characterization of chicken bone marrow-derived dendritic cells. *Immunology.* (2010) 129:133–45. doi: 10.1111/j.1365-2567.2009.03129.x

43. Kaspers B, Lillehoj HS, Lillehoj EP. Chicken macrophages and thrombocytes share a common cell surface antigen defined by a monoclonal antibody. *Vet Immunol Immunopathol.* (1993) 36:333–46. doi: 10.1016/0165-2427(93)90029-4

44. Rothwell CJ, Vervelde L, Davison TF. Identification of chicken Bu-1 alloantigens using the monoclonal antibody AV20. *Vet Immunol Immunopathol.* (1996) 55:225–34. doi: 10.1016/s0165-2427(96)05635-8

45. Kameka AM, Haddadi S, Jamaldeen FJ, Moinul P, He XT, Nawazdeen FHP, et al. Clodronate treatment significantly depletes macrophages in chickens. *Can J Vet Res.* (2014) 78:274–82. Available online at: http://www.ncbi.nlm.nih.gov/pmc/articles/PMC4170766/

46. Li Z, Nestor KE, Saif YM, Fan Z, Luhtala M, Vainio O. Cross-reactive anti-chicken CD4 and CD8 monoclonal antibodies suggest polymorphism of the turkey CD8alpha molecule. *Poult Sci.* (1999) 78:1526–31. doi: 10.1093/ps/78.11.1526

47. Lippincott-Schwartz J, Fambrough DM. Lysosomal membrane dynamics: structure and interorganellar movement of a major lysosomal membrane glycoprotein. *J Cell Biol.* (1986) 102:1593–605. doi: 10.1083/jcb.102.5.1593

48. de Geus ED, Jansen CA, Vervelde L. Uptake of particulate antigens in a nonmammalian lung: phenotypic and functional characterization of avian respiratory phagocytes using bacterial or viral antigens. *J Immunol.* (2012) 188:4516–26. doi: 10.4049/jimmunol.1200092

49. Martin M. Cutadapt removes adapter sequences from high-throughput sequencing reads. *EMBnet J.* (2011) 17:10–12. doi: 10.14806/ej.17.1.200

50. Dobin A, Davis CA, Schlesinger F, Drenkow J, Zaleski C, Jha S, et al. STAR: ultrafast universal RNA-seq aligner. *Bioinformatics.* (2013) 29:15–21. doi: 10.1093/bioinformatics/bts635

51. Liao Y, Smyth GK, Shi W. featureCounts: an efficient general purpose program for assigning sequence reads to genomic features. *Bioinformatics.* (2014) 30:923–30. doi: 10.1093/bioinformatics/btt656

52. Robinson MD, Oshlack A. A scaling normalization method for differential expression analysis of RNA-seq data. *Genome Biol.* (2010) 11:R25. doi: 10.1186/gb-2010-11-3-r25

53. Spinelli L, Carpentier S, Montañana Sanchis F, Dalod M, Vu Manh TP. BubbleGUM: automatic extraction of phenotype molecular signatures and comprehensive visualization of multiple Gene Set Enrichment Analyses. *BMC Genomics.* (2015) 16:814. doi: 10.1186/s12864-015-2012-4

54. Vu Manh TP, Elhmouzi-Younes J, Urien C, Ruscanu S, Jouneau L, Bourge M, et al. Defining mononuclear phagocyte subset homology across several distant warm-blooded vertebrates through comparative transcriptomics. *Front Immunol.* (2015) 6:299. doi: 10.3389/fimmu.2015.00299

55. Schusser B, Collarini EJ, Yi H, Izquierdo SM, Fesler J, Pedersen D, et al. Immunoglobulin knockout chickens via efficient homologous recombination in primordial germ cells. *Proc Natl Acad Sci USA.* (2013) 110:20170–5. doi: 10.1073/pnas.1317106110

56. Miller JC, Brown BD, Shay T, Gautier EL, Jojic V, Cohain A, et al. Deciphering the transcriptional network of the dendritic cell lineage. *Nat Immunol.* (2012) 13:888–99. doi: 10.1038/ni.2370

57. Bagadia P, Huang X, Liu TT, Durai V, Grajales-Reyes GE, Nitschke M, et al. An Nfil3-Zeb2-Id2 pathway imposes Irf8 enhancer switching during cDC1 development. *Nat Immunol.* (2019) 20:1174–85. doi: 10.1038/s41590-019-0449-3

58. Boulet S, Daudelin JF, Odagiu L, Pelletier AN, Yun TJ, Lesage S, et al. The orphan nuclear receptor NR4A3 controls the differentiation of monocyte-derived dendritic cells following microbial stimulation. *Proc Natl Acad Sci USA.* (2019) 116:15150–9. doi: 10.1073/pnas.1821296116

59. Satpathy AT, Kc W, Albring JC, Edelson BT, Kretzer NM, Bhattacharya D, et al. Zbtb46 expression distinguishes classical dendritic cells and their committed progenitors from other immune lineages. *J Exp Med.* (2012) 209:1135–52. doi: 10.1084/jem.20120030

60. Meredith MM, Liu K, Darrasse-Jeze G, Kamphorst AO, Schreiber HA, Guermonprez P, et al. Expression of the zinc finger transcription factor zDC (Zbtb46, Btbd4) defines the classical dendritic cell lineage. *J Exp Med.* (2012) 209:1153–65. doi: 10.1084/jem.20112675

61. Sieweke MH, Tekotte H, Frampton J, Graf T. MafB is an interaction partner and repressor of Ets-1 that inhibits erythroid differentiation. *Cell.* (1996) 85:49–60. doi: 10.1016/s0092-8674(00)81081-8

62. Bakri Y, Sarrazin S, Mayer UP, Tillmanns S, Nerlov C, Boned A, et al. Balance of MafB and PU.1 specifies alternative macrophage or dendritic cell fate. *Blood.* (2005) 105:2707–16. doi: 10.1182/blood-2004-04-1448

63. Luchin A, Suchting S, Merson T, Rosol TJ, Hume DA, Cassady AI, et al. Genetic and physical interactions between Microphthalmia transcription factor and PU.1 are necessary for osteoclast gene expression and differentiation. *J Biol Chem.* (2001) 276:36703–10. doi: 10.1074/jbc.M106418200

64. DeKoter RP, Singh H. Regulation of B lymphocyte and macrophage development by graded expression of PU.1. *Science.* (2000) 288:1439-41. doi: 10.1126/science.288.5470.1439

65. Rehli M, Lichanska A, Cassady AI, Ostrowski MC, Hume DA. TFEC is a macrophage-restricted member of the microphthalmia-TFE subfamily of basic helix-loop-helix leucine zipper transcription factors. *J Immunol.* (1999) 162:1559–65

66. Scott CL, T'Jonck W, Martens L, Todorov H, Sichien D, Soen B, et al. The Transcription factor ZEB2 is required to maintain the tissue-specific identities of macrophages. *Immunity.* (2018) 49:312–25.e5. doi: 10.1016/j.immuni.2018.07.004

67. Kohyama M, Ise W, Edelson BT, Wilker PR, Hildner K, Mejia C, et al. Role for Spi-C in the development of red pulp macrophages and splenic iron homeostasis. *Nature.* (2009) 457:318–21. doi: 10.1038/nature07472

68. Larsen FT, Bed'Hom B, Guldbrandtsen B, Dalgaard TS. Identification and tissue-expression profiling of novel chicken c-type lectin-like domain containing proteins as potential targets for carbohydrate-based vaccine strategies. *Mol Immunol.* (2019) 114, 216–25. doi: 10.1016/j.molimm.2019.07.022

69. Miyanishi M, Tada K, Koike M, Uchiyama Y, Kitamura T, Nagata S. Identification of Tim4 as a phosphatidylserine receptor. *Nature.* (2007) 450:435–9. doi: 10.1038/nature06307

70. Verma R, Jaiswal H, Chauhan KS, Kaushik M, Tailor P. Cutting edge: ACVRL1 signaling augments CD8α^+ dendritic cell development. *J Immunol.* (2016) 197:1029–34. doi: 10.4049/jimmunol.1501849

71. Forni D, Cagliani R, Tresoldi C, Pozzoli U, De Gioia L, Filippi G, et al. An evolutionary analysis of antigen processing and presentation across different timescales reveals pervasive selection. *PLoS Genet.* (2014) 10:e1004189. doi: 10.1371/journal.pgen.1004189

72. Theisen DJ, Davidson JT, Briseno CG, Gargaro M, Lauron EJ, Wang Q, et al. WDFY4 is required for cross-presentation in response to viral and tumor antigens. *Science.* (2018) 362:694–9. doi: 10.1126/science.aat5030

73. Gautier EL, Shay T, Miller J, Greter M, Jakubzick C, Ivanov S, et al. Gene-expression profiles and transcriptional regulatory pathways that underlie the identity and diversity of mouse tissue macrophages. *Nat Immunol.* (2012) 13:1118–28. doi: 10.1038/ni.2419

74. Sekelova Z, Stepanova H, Polansky O, Varmuzova K, Faldynova M, Fedr R, et al. Differential protein expression in chicken macrophages and heterophils *in vivo* following infection with Salmonella Enteritidis. *Vet Res.* (2017) 48:35. doi: 10.1186/s13567-017-0439-0

75. Rooijen NV, Sanders A. Liposome mediated depletion of macrophages: mechanism of action, preparation of liposomes and applications. *J Immunol Methods.* (1994) 174:83–93. doi: 10.1016/0022-1759(94)90012-4

76. Hume DA. The mononuclear phagocyte system. *Curr Opin Immunol.* (2006) 18:49–53. doi: 10.1016/j.coi.2005.11.008

77. Sauter KA, Pridans C, Sehgal A, Bain CC, Scott C, Moffat L, et al. The MacBlue binary transgene (csf1r-gal4VP16/UAS-ECFP) provides a novel marker for visualisation of subsets of monocytes, macrophages and dendritic cells and responsiveness to CSF1 administration. *PLoS ONE.* (2014) 9:e105429. doi: 10.1371/journal.pone.0105429

78. Jeurissen SH. The role of various compartments in the chicken spleen during an antigen-specific humoral response. *Immunology.* (1993) 80:29–33.

79. Mast J, Goddeeris BM. CD57, a marker for B-cell activation and splenic ellipsoid-associated reticular cells of the chicken. *Cell Tissue Res.* (1998) 291:107–15. doi: 10.1007/s004410050984

80. Wu Z, Harne R, Chintoan-Uta C, Hu TJ, Wallace R, MacCallum A, et al. Regulation and function of macrophage colony-stimulating factor (CSF1) in the chicken immune system. *Dev Comp Immunol.* (2019) 105:103586. doi: 10.1016/j.dci.2019.103586

81. Nagy N, Biro E, Takacs A, Polos M, Magyar A, Olah I. Peripheral blood fibrocytes contribute to the formation of the avian spleen. *Dev Dyn.* (2005) 232:55–66. doi: 10.1002/dvdy.20212

82. Cinamon G, Zachariah MA, Lam OM, Foss FW, Cyster JG. Follicular shuttling of marginal zone B cells facilitates antigen transport. *Nat Immunol.* (2008) 9:54–62. doi: 10.1038/ni1542

83. Jeurissen SHM. Structure and function of the chicken spleen. *Res Immunol.* (1991) 142:352–5. doi: 10.1016/0923-2494(91)90090-6

84. Huynh KK, Eskelinen EL, Scott CC, Malevanets A, Saftig P, Grinstein S. LAMP proteins are required for fusion of lysosomes with phagosomes. *EMBO J.* (2007) 26:313–24. doi: 10.1038/sj.emboj.7601511

85. Yu K, Gu MJ, Pyung YJ, Song KD, Park TS, Han SH, et al. Characterization of splenic MRC1^{hi}MHCII^{lo} and MRC1^{lo}MHCII^{hi} cells from the monocyte/macrophage lineage of White Leghorn chickens. *Vet Res.* (2020) 51:73. doi: 10.1186/s13567-020-00795-9

86. Stahl P, Schlesinger PH, Sigardson E, Rodman JS, Lee YC. Receptor-mediated pinocytosis of mannose glycoconjugates by macrophages: characterization and evidence for receptor recycling. *Cell.* (1980) 19:207–15. doi: 10.1016/0092-8674(80)90402-x

87. Nakano H, Moran TP, Nakano K, Gerrish KE, Bortner CD, Cook DN. Complement receptor C5aR1/CD88 and dipeptidyl peptidase-4/CD26 define distinct hematopoietic lineages of dendritic cells. *J Immunol.* (2015) 194:3808–19. doi: 10.4049/jimmunol.1402195

88. Ikushima H, Munakata Y, Ishii T, Iwata S, Terashima M, Tanaka H, et al. Internalization of CD26 by mannose 6-phosphate/insulin-like growth factor II receptor contributes to T cell activation. *Proc Natl Acad Sci USA.* (2000) 97:8439–44. doi: 10.1073/pnas.97.15.8439

89. Naito Y, Takagi T, Higashimura Y. Heme oxygenase-1 and anti-inflammatory M2 macrophages. *Arch Biochem Biophys.* (2014) 564:83–8. doi: 10.1016/j.abb.2014.09.005

90. Hey YY, O'Neill HC. Murine spleen contains a diversity of myeloid and dendritic cells distinct in antigen presenting function. *J Cell Mol Med.* (2012) 16:2611–9. doi: 10.1111/j.1582-4934.2012.01608.x

91. Pridans C, Holmes ML, Polli M, Wettenhall JM, Dakic A, Corcoran LM, et al. Identification of Pax5 target genes in early B cell differentiation. *J Immunol.* (2008) 180:1719–28. doi: 10.4049/jimmunol.180.3.1719

92. Tamura T, Tailor P, Yamaoka K, Kong HJ, Tsujimura H, O'Shea JJ, et al. IFN regulatory factor-4 and−8 govern dendritic cell subset development and their functional diversity. *J Immunol.* (2005) 174:2573–81. doi: 10.4049/jimmunol.174.5.2573

93. Honma K, Udono H, Kohno T, Yamamoto K, Ogawa A, Takemori T, et al. Interferon regulatory factor 4 negatively regulates the production of proinflammatory cytokines by macrophages in response to LPS. *Proc Natl Acad Sci USA.* (2005) 102:16001–6. doi: 10.1073/pnas.0504226102

Conflict of Interest: The authors declare that the research was conducted in the absence of any commercial or financial relationships that could be construed as a potential conflict of interest.